UNIVERSITY OF MINNESOTA
ST. ANTHONY FALLS HYDRAULIC LABORATORY

Project Report No. 95

MODEL STUDIES OF CHLORINE SOLUTION DISPERSION IN TURBULENT PIPE FLOW

by
J. W. Hayden

Prepared for
HARZA ENGINEERING COMPANY
and the
Metropolitan Water District of Southern California

June 1968
Minneapolis, Minnesota

University of Minnesota
ST. ANTHONY FALLS HYDRAULIC LABORATORY

Project Report No. 95

MODEL STUDIES OF CHLORINE SOLUTION DISPERSION IN TURBULENT PIPE FLOW

by
J. W. Hayden

Prepared for
HARZA ENGINEERING COMPANY
and the
Metropolitan Water District of Southern California

June, 1968
Minneapolis, Minnesota

C/

CONTENTS

A. Description of Model and Appurtenances

Because of the two objectives given above, the test program was divided into two parts. First, a detailed study was made of a small full-scale nozzle in a water tunnel (Nozzle Model) in order to determine the nozzle characteristics from both the hydraulic and vibration viewpoint. Second, the overall dispersion pattern downstream from the injection point was studied in a pipeline; this was called "Dispersion Model."

Nozzle Model: An overall view of this model in operation is shown in Photo 1. Water, marked with potassium permanganate, is being injected through the nozzle. The purpose of this model was to make as nearly full-scale tests as possible of the injection nozzle. The tunnel used is 13 in. high and 12 in. wide throughout the test section and permitted velocities up to about 16 fps. The stream, before entering the test section, is contracted at the top in such a way that the velocity is higher at the top of the test section than at the bottom. Thus, the flow in the tunnel represents the portion of the velocity profile near the wall of a larger pipe. The graph in Fig. 1 shows a comparison of the measured profiles in the tunnel with calculated turbulent profiles for several representative pipes.

The dispersion tests associated with the Nozzle Model were conducted using either a 2 in. I.D. copper pipe or the same pipe fitted with a streamlined outer case (see Photo 2). By always extending the nozzle 6 in. into the tunnel, the injected fluid entered the portion of the tunnel in which the velocity profile was in substantial agreement with that of a much larger pipe (see Fig. 1). Further insertion would have been unwise because the opposite wall would have been approached too closely and interference effects would have resulted.

In performing the vibration tests it was not possible to concurrently pass flow through the nozzle. Thus a short cylindrical nozzle was connected to a dynamometer system as shown in Photo 3. Two nozzles were tested, an open-end copper tube and a light-weight, closed-end lucite tube, to determine if the vibrational characteristics at the nozzle would alter due to a change in mass or configuration of the end of the nozzle. Both the forces acting on the nozzle due to the action of the water flowing past the nozzle and the frequency of the nozzle vibration were measured.

Dispersion Model: The dispersion model apparatus consists of a 183 ft long, 10 in. diameter, galvanized iron pipeline with transparent test sections located along its length (see Photos 4 and 5 which show, respectively, a view of the panel board and an overall view of the pipe). An 89 ft long entrance length is provided to establish a normal, turbulent velocity profile in the 10 in. pipe. The velocity profile was measured at the Pitot station at the end of the entrance length using a Pitot cylinder. The measured and calculated velocity profiles for the 10 in. pipe are compared on Fig. 2.

A lucite ring fitted with several injection nozzles for injection of chlorine solution was located just upstream of the first observation section following the entrance length. Injection was through a 3/8 in. I.D. tube or tubes extended into the pipe. No attempt was made to model the nozzle in this apparatus except as noted in the section, Scale Relationhsip and Hydraulic Similarity. Studies were made with several injector configurations.

The additional observation sections, as well as the first one, were used for observing the dispersion of dye in the pipeline. Chlorine dispersion was measured by titration using equipment provided by MWD. Samples for titration were obtained through the Pitot cylinders similar to those used for measuring velocity profiles. These could be inserted at any of the Pitot stations spaced along the pipe downstream from the injection point.

B. Scale Relationship and Hydraulic Similarity

The mixing of two essentially identical fluid streams (one containing a small percentage of chlorine) in turbulent pipe flow is due mainly to mass transfer. The rate of mass transfer in a moving fluid is primarily dependent on the degree of turbulence that exists within the flow. In performing tests in which the turbulence characteristics of the fluid are important, dynamic similarity is obtained for geometrically similar structures when the Reynolds number in the prototype and model are equal. Thus

$$R_{prototype} = R_{model}$$

and if water is the fluid flowing in both systems, then

$$V_p D_p = V_m D_m$$

where V is velocity and D is pipe diameter and the subscripts p and m refer to prototype and model, respectively.

Because of the physical size of the pipelines of interest to MWD, the velocities through the 10 in. diameter model would range up to 200 fps if the Reynolds number of the two systems were to be equal. It would have been difficult to achieve velocities exceeding 20 fps; thus, the tests were instead conducted at velocities comparable to those of interest to MWD (5, 10, and 15 fps). Even though the Reynolds number was approximately an order of magnitude less in the model than in the prototype, the range of the model Reynolds number was from 2×10^5 up to 6×10^5; dynamic similarity with reference to dispersion characteristics, although not completely achieved, would be essentially the same in both systems because both are operating well into the turbulent flow region.

In conducting the pipeline tests, the size and length of the injection nozzle were selected so that the ratios of nozzle diameter/pipe diameter (d/D) and nozzle length/pipe diameter (l/D) would be representative of those used by the MWD in their prototype installations. A 3/8 in. I.D. nozzle injecting normal to the flow through the 10 in. I.D. pipeline was used for all the tests. The injector was extended either 3/4 in. or 1-1/2 in. into the pipe. Thus, the following table can be developed:

Experimental Conditions			Prototype Conditions		
Pipe Dia. inches	Injector		Pipe Dia. feet	Injector	
	Dia. inches	Length inches		Dia. inches	Length inches
10	3/8	3/4	9	4	8
10	3/8	1-1/2	9	4	16
10	3/8	3/4	18	8	16
10	3/8	1-1/2	18	8	32

However, based on the tests using a single or double injector injecting on the horizontal diameter, an ℓ/D ratio as low as .05 should be satisfactory. As a result, an injector length of 6 in. and 12 in. should be satisfactory for pipes 9 ft and 18 ft in diameter respectively.

II. EXPERIMENTAL RESULTS

Results of studies of the dispersion of chlorine solution injected into turbulent pipe flow are described below. The experiments dealing with the testing of a small, full-scale nozzle in the water tunnel are described first. The test results of the dispersion of the injected chlorine solutions downstream from the injection point are described in the second portion of the discussion.

A. Nozzle Model

The purpose of the nozzle model test was to make as nearly a full-scale test as possible of an injection nozzle. A nozzle with a 2 in. I.D. was extended 6 in. into the test tunnel. The tunnel, as described earlier, was designed so that the velocity profile in the tunnel would represent the velocity profile near the wall of a much larger pipe. Thus, the observed dispersion patterns and dynamic forces would be similar to those that would occur if the nozzle were inserted 6 in. into a pipe 2.5 to 10 ft in diameter, based on the recommendation that the nozzle length be between .20 and .05 times the pipe diameter.

The distance from the centerline of the injectors to the downstream edge of the tunnel is approximately 3 ft. The dispersion that occurs within the first few feet of an injection nozzle is shown in Photos 6 through 14. The dispersion in prototype pipes would be similar to that shown in the photographs for a wide range of pipe diameters, assuming equal flow and injection velocities. Thus, for example, the photographs show the dispersion that takes place within 1/2 or 1/4 of a pipe diameter for a 6 ft or 12 ft diameter pipe, respectively. In addition to photographic data, both the vibratory forces acting on the nozzle and the frequency of the nozzle vibrations were measured.

Dye Injection Pattern: A series of tests was conducted with the model configuration shown in Photo 1, using either a cylindrical or streamlined injector. The results of the photographic study (see Photos 6 through 14 for typical results) indicate that good dispersion of the injected fluid is obtained over a wide range of tunnel and injector velocities. The results of the photographic study also indicate that the dispersion pattern is essentially the same with or without streamlining. (See Photos 12 and 13 for comparison.) Whenever the ratio of injector mean velocity to pipe mean velocity (V_i/V_p) is the same, the dye dispersion pattern is similar, as shown by comparing Photos 11 and 12 for the cylindrical nozzle with Photos 13 and 14 for the streamlined nozzle. Thus, it can be concluded that the dispersion of the dye is little affected by the shape of the injector nozzle, provided normal injection is always used. For equal V_i/V_p ratios the dye dispersion was similar for all pipe velocities within the range of the velocities tested (up to 15 fps).

It was noted that for those tests in which both the injector and tunnel velocity were lowest, the injected fluid formed a thin film on the downstream side of the injector extending from the open end of the injector almost to the wall for both the streamlined and the cylindrical injectors (see Photos 15 and 16). This effect occurred to a somewhat smaller degree for the streamlined nozzle. The existence of the film of injected fluid suggests that it would be a good practice to use injector velocities equivalent to 1/2 or more of the pipe velocities.

Vibration Analysis: With the nozzle as originally designed it was not possible to detect any vibratory forces. This result was due to the massiveness of the system and the type of supports used. Thus, a lighter nozzle and new support system were designed and tested.

It was necessary to use a short nozzle connected directly to a dynamometer system, as shown in Photos 3, 17, and 18 to obtain vibration data. The nozzles were 2 in. I.D. and extended 6 in. into the tunnel. Using this design, it was not possible to pass flow through the nozzle while the vibration tests were being conducted. Thus, two nozzles were tested, a light-weight closed-end lucite tube (Photo 17) and an open-end copper tube (Photo 18), to determine if the vibration characteristics would change due to a change in the configuration of the end of the nozzle or the mass of the nozzle.

In the tests, the assumption was made that if a critical condition with regard to the magnitude of the forces or the frequency of vibration occurred, this would be apparent with or without flow through the nozzle. This appears to be a reasonable assumption because the only forces produced by the flow within the nozzle are along its axis and cannot contribute to the transverse forces or vibrations. The water in the tube acts as an additional mass; therefore, tests were made with tubes of different masses. There was no measurable effect, as shown in Fig. 3.

Furthermore, the experimental results showed that the forces acting on the nozzle were of such small magnitude (extrapolation yields a value of less than 10 lbs. for velocity of 15 fps) that even if the assumption were in error and the occurrence of flow through the nozzle were to increase the force by a factor of ten (an extremely unlikely result), such increased force would still be too small to cause damage to the nozzle. With such small forces the only possibility of damage to the nozzle would be the occurrence of resonance. For this reason vibrational frequencies were also analyzed.

On Fig. 4 the frequency of the existing vibratory force is compared to the frequency that would result from vortex shedding. Investigations have shown that the Strouhol number $(S = \frac{\eta D}{V}$ where η is the frequency, D the cylinder diameter, and V the flow velocity) is a constant, approximately 0.21, for Reynolds numbers from 10^3 up to approximately 10^6.* Thus for the system tested the vortex shedding frequency can be calculated by

$$\eta = \frac{.21 \times V}{\frac{2.125}{12}} = 1.19\ V\ \left(\frac{ft}{sec}\right) \qquad [1]$$

The equation $\eta = 1.19\ V$ has been plotted on Fig. 4 for comparison with the experimental data. For tunnel velocities of less than 8 fps the agreement between Eq. 1 and the data is reasonably good, thus indicating that vortex shedding is the primary cause of the vibratory force. However, at higher velocities the correlation is not as satisfactory. The increase in

*Roshko, A., "Experiments on the Flow Past a Circular Cylinder at Very High Reynolds Numbers," Journal of Fluid Mechanics, Vol. 10, Part 3, May 1961.

vibratory frequency at higher velocities may have been caused by one of two factors: (1) the flow past the injector tube is three-dimensional instead of two-dimensional as assumed in Eq. 1, or (2) the record from the Sanborn recorder for high tunnel velocities was difficult to analyze due to the presence of extraneous vibratory frequencies. Again it should be observed that both the copper and lucite tubes vibrate at essentially the same frequency.

For the velocity range of interest to MWD (5 to 15 fps), the forced vibrational frequency acting on the nozzle tested was from 6 to approximately 20 cps; the natural frequency of the thin-walled copper tube and dynamometer system, which was mounted very flexibly, was 75 cps. Since the forced frequency must reach at least half the natural frequency to have a chance for resonance to occur, resonance did not occur under the test conditions. For the prototype system, the forced vibrations, which would be caused by vortex shedding, would range up to a maximum of approximately 18 cps, based on a Strouhol No. = 0.21. With the nozzles inserted as they are in the prototype pipes, the natural frequency would be at least several hundred cps. Thus, it is not conceivable that resonance could be introduced in the prototype nozzles either with or without flow through the nozzle.

It should be noted that the first observations of the full-scale model were made with water flowing through the nozzle, but the nozzle was more rigidly attached to the tunnel wall than in the later tests, wherein the nozzles were supported by the dynamometer. Although there was some small vibration in the earlier tests, the vibration was associated with the pump producing flow through the nozzle; there was no sign of resonance or change in vibration with or without flow through the nozzle.

Had the system used created any doubt about the prototype installation, a more complicated dynamometer capable of handling flow through the nozzle would have been built. However, in light of the previous discussion, it was quite apparent that any more sophisticated measurements would be unnecessary.

Based on the large scale model tests, the following conclusions can be made:

1. The chlorine dispersion pattern near the injector would be relatively unaffected by the streamlining of the injector.

2. The injector velocity should be a minimum of 1/2 the pipe velocity or 2-1/2 fps, whichever is greater.

3. The vibratory forces acting on a cylindrical injector would be of such small magnitude and in a frequency range far enough removed from the natural frequency of the prototype injector that damage to an injector is unlikely to result from dynamic forces.

Thus, it can be concluded that the cylindrical nozzle injecting normal to the main flow would be satisfactory with respect to both the resulting diffusion pattern, as well as the dynamic forces acting on the nozzle. The streamlined nozzle has little or no advantage with respect to either of these considerations.

B. Dispersion Model

Preliminary tests consisted of velocity profile measurement (Fig. 2), friction factor determination (Fig. 5), and flow meter calibration in the 10 in. pipeline. The next tests involved measurement of the diffusion of water containing approximately 1500 ppm potassium permanganate injected into the pipe. Concentration profiles of the water marked with the potassium permanganate were obtained across the horizontal plane at pipe length to pipe diameter ratios (L/D) of 7.2, 30, and 61 downstream from the point of injection. Injection of the dye was at 3/4 in. and 1-1/2 in. from the wall of the 10 in. diameter pipe. The dye was injected on the horizontal diameter normal to, and at the same velocity as, the flow in the 10 in. pipe. These data are shown in Figs. 6 through 8.

Earlier tests with potassium permanganate using tap water had indicated that adequate data could be obtained before substantial oxidation had taken place; however, when the permanganate solution was injected into the natural river water flowing through the 10 in. pipe, the reaction was much more rapid and it became difficult to obtain consistent data; the scatter of data on Fig. 9 is a result of this problem. Thus, a series of tests was conducted using chlorine solution as the injected fluid.

The first chlorine tests were conducted using a single nozzle injecting on the horizontal diameter of the pipe. The results of the chlorination studies using one injector are shown in Figs. 10 and 11 and in one of the curves in Fig. 14. The following conclusions can be drawn from these figures.

1. The chlorine concentration profiles are essentially the same for the injection tube projecting either 3/4 in. ($\ell/D = 0.075$) or 1-1/2 in ($\ell/D = 0.15$) into the 10 in. diameter pipe. Thus once the injection tube is extended into the main core of the flow, that is, the central portion of the pipe throughout which the velocity is relatively constant for turbulent flow (see Fig. 2), the diffusion of the injected fluid is independent of the distance which the injection tube extends into the pipe over a range of injection tube lengths of 0.05 diameter, as a minimum, up to approximately 0.20 diameter. Thus, for example, an injection tube length of 6 in. should be adequate for a pipe 10 ft in diameter. From Figs. 10 and 11, it can be seen that the point of maximum concentration was always (with few exceptions at large L/D values) near the wall on the same side as the injection tube, indicating that the presence of the injection tube strongly influences the diffusion of the injected fluid for L/D values of 60 or less.

2. For similar flow conditions, i.e., constant V_i/V_p ratio, the concentration profiles are independent of the velocity in the 10 in. pipe for the range of variables tested.

3. The length of pipe (expressed in terms of L/D values) necessary to obtain various degrees of uniformity of concentration of injected fluid may be determined from Fig. 14. The degree of uniformity is expressed as the minimum concentration divided by the maximum concentration (C_{min}/C_{max}) measured across the diameter of the pipe. For example, if a variation from a minimum to a maximum chlorine concentration across the diameter of 3 ppm to 4 ppm, respectively, were acceptable, the measuring point would have to be approximately 105 pipe diameters downstream from the

injection point. It should be noted that for these tests this result is independent of both the pipe velocity and the distance the injector extends into the pipe.

If a single injector were used in a prototype installation, the distance between the injection point and the point at which relatively uniform chlorine concentration across the pipe would exist was considered to be excessive (perhaps 2000 ft for an 18 ft diameter pipe). Thus, tests were conducted using two injectors, one on each side of the pipe. The results, using two injectors, are shown in Figs. 12 and 13. The conclusions that were made for a single injector system are true for a double injector system as well, except for one important consideration: the length required to achieve a given degree of mixing has been considerably reduced. From Fig. 14, it can be seen that the "mixing length" for the double injector system is only approximately 30 per cent of that required using a single injector system. This means that the distance from the point of injection to a monitoring point, or to the location of any structural component that would be susceptible to damage from excessive chlorine concentrations, could be reduced by a factor of 3-1/3 if double injectors were used.

Having observed a significant reduction in the "mixing length" required to reach a given uniformity of concentration across the horizontal diameter of the pipe in going from one to two injectors, it was decided that a scheme using four injectors, as shown in Fig. 15a should be tested to determine if the "mixing length" would again be significantly reduced. The detailed chlorine concentration profiles using four injectors are shown in Figs. 16 and 17. Again, as in all previous tests, the chlorine concentration profiles are essentially the same for the injection tubes projecting either 3/4 in. or 1-1/2 in. into the 10 in. diameter pipe and for similar flow conditions, i.e., constant V_i/V_p ratio, for the range of variables tested.

Fig. 20 shows that there was not a further significant reduction in the L/D valve necessary to obtain a given C_{min}/C_{max} ratio across the horizontal diameter using the four injector system shown in Fig. 15a. Thus the four injector system would be only slightly better than a two injector system for obtaining a rapid dispersal of the injected fluid throughout the pipe cross section.

Tests were also conducted using the nozzle configurations shown in Figs. 15b and 15c. The concentration profiles, shown in Figs. 18 and 19, may be interpreted as representing the horizontal and vertical profiles for two injectors located 30 and 38 degrees above the horizontal diameter respectively. These tests were conducted to determine if satisfactory chlorine dispersion could be obtained with the configuration shown in Fig. 15b. If this were possible, the physical size of the prototype structure surrounding the injection point could be considerably reduced. However, previous tests using a single injector indicated that there would be a "dead spot" at the bottom of the pipe. To examine whether this possibility existed for two injectors near the top of the pipe, the tests using the configuration shown in Fig. 15c were conducted. These tests were conducted with the injector tube extended only 3/4 in. into the pipe $(\frac{\ell}{D} = .075)$, because in prototype installations the injector tubes will most often be of minimum length $(\frac{\ell}{D} = .05)$, and a length of both 3/4 in. and 1-1/2 in. produces essentially identical results. As anticipated (see Fig. 19), a point of low chlorine concentration does exist at what would be the bottom of the pipe for a considerable distance downstream from the injection point.

On Fig. 20 the results of all the tests conducted are compared. The curves labelled 4 and 5 represent the horizontal and vertical profiles, respectively, for the injector configuration shown in Fig. 15b. The dispersion in the vertical plane is not substantially different than that obtained using a single injector. Thus, it is concluded that the use of two injectors on the horizontal diameter for producing relatively uniform concentrations in a short distance downstream from the injection point would be more satisfactory than the use of the configuration shown in Fig. 15b.

Throughout the entire experimental program one factor became clearly evident: that the dispersion pattern is strongly influenced by the presence of the injection nozzle. This single factor would make it difficult, if not impossible, to predict the chlorine concentration profiles downstream of the injection point by analytical means. With few exceptions, throughout the entire test program the highest chlorine concentration always occurred at the wall of the pipe. This phenomenon is apparently caused by the injected fluid flowing into the wake area behind the nozzle and then radially outward around the pipe wall, as sketched in Fig. 21.

The injected fluid being drawn into the wake could cause higher chlorine concentrations to reach the wall several pipe diameters downstream from the injection point. However, it is doubtful if the fluid reaching the wall would normally exceed 1/50 of the concentration of the injected fluid. The concentration at the first measuring station in these tests (7.2 diameter downstream from the injection point) did not exceed 1/100 of injected concentration when more than one injector was used to achieve a uniform residual concentration of 2 to 4 ppm. Thus, even though the injected fluid is drawn near the wall, the process is not likely to cause excessive chlorine concentrations at the wall, and in fact the secondary flow caused by the nozzle would actually accelerate the dispersion process.

III. CONCLUSIONS

It can be concluded that a cylindrical nozzle injecting normal to the main flow would be a satisfactory design with respect to both the resulting diffusion pattern as well as the dynamic forces acting on the nozzle. However, the following criteria should be satisfied by the prototype nozzle:

1. The injector velocity should equal or exceed 2-1/2 fps or 1/2 the large pipe velocity, whichever is greater.
2. The injector, or injectors, should extend into the large pipe a length equal to or greater than 0.05 times the diameter of the pipe.

Based on the overall results obtained using various numbers and locations of injectors (see Fig. 20), two injectors placed on the horizontal diameter appears to be the best solution. This system results in a relatively rapid dispersion of the injected chlorine solution without the additional construction cost and operational complexity that the use of four injectors would require.

LIST OF PHOTOS

PHOTO 1 (Serial No. 176-73) Overall view of tunnel showing the head section, and tailwater section. Dyed water is being injected through the streamlined nozzle. Both the tunnel and injector velocities are 5 fps.

PHOTO 2 (Serial No. 176-72) Streamlined injection nozzle formed by fitting a 6 in. long wood housing over a 2 in. I.D. copper tube.

PHOTO 3 (Serial No. 176-45) Overall view of vibration test equipment. Cylindrical copper tube injection nozzle, 2 in. I.D., 6 in. long, is installed in the tunnel (background). The vibrational force and frequency are being recorded on a Sanborn recorder (foreground).

PHOTO 4 (Serial No. 176-41) Close-up view of a portion of the panel board used to control the flow to the injection nozzles, the viewing box adjacent to the point of injection (dyed water is being injected), and the operator titrating a sample taken from the 10 in. diameter pipe.

PHOTO 5 (Serial No. 176-31) Lengthwise view of the 10 in. diameter pipeline test facility. The manometers used to measure the friction loss and the viewing box adjacent to the injection point are visible in the foreground.

PHOTO 6 (Serial No. 176-7) In Photos 6 through 14 water marked with potassium permanganate is being injected into the water tunnel through a 2 in. I.D., 6 in. long injector nozzle for various flow conditions. In Photo 6 the tunnel velocity is 5 fps and the injector velocity is 1.8 fps. The general dispersion pattern downstream from the injector is shown. A thin film of dyed water (injected fluid) formed on a vertical plane on the downstream side of the nozzle. Exposure time for Photos 6 through 11 is 1/4 sec.

PHOTO 7 (Serial No. 176-9) Tunnel velocity is 5 fps, but the injector velocity has been increased to 3.6 fps. Injected fluid does not collect on the downstream side of the nozzle for these conditions.

PHOTO 8 (Serial No. 176-11) Injector velocity further increased to 5.4 fps; tunnel velocity maintained at 5 fps. Observe that as the injection velocity is increased from 1.8 to 5.4 fps (Photos 6, 7, and 8), the injected fluid approaches more closely the top boundary of the tunnel. Thus, for pipe flow the injected fluid would be thrust away from the pipe wall and further into the center core of the flow, as the injection velocity was increased.

PHOTO 9 (Serial No. 176-13) Tunnel velocity has been increased to 10 fps; injector velocity is 3.6 fps.

PHOTO 10 (Serial No. 176-15) Tunnel velocity is 10 fps; injector velocity is 7.2 fps.

PHOTO 11 (Serial No. 176-17) Tunnel velocity is 10 fps; injector velocity is 10.8 fps. Comparing Photos 6 and 9, Photos 7 and 10, and Photos 8 and 11, note the similarity of the dispersion pattern when the V_I/V_T ratio is the same.

PHOTO 12 (Serial No. 176-49) In this photo and Photo 13 both the tunnel and injector velocities are 5 fps. The photographs were taken with an exposure time of 1/100 sec so that the details of the dispersion pattern for the cylindrical (Photo 12) and streamlined nozzle (Photo 13) could be compared. Each picture shows the dispersion pattern within the first 3 ft downstream of the injection point. Note the similarity of the dispersion patterns.

PHOTO 13 (Serial No. 176-52) Dispersion pattern for streamlined injection nozzle. Tunnel and injection velocities are 5 fps.

PHOTO 14 (Serial No. 176-67) Dispersion pattern for streamlined injection nozzle with tunnel and injection velocity of 10 fps. Note the similarity of the dispersion pattern in this photo and Photos 12 and 13. Thus, whenever the ratio V_I/V_T is the same as it is for Photos 12, 13, and 14, the dispersion within the first few feet downstream of the injection nozzle will be essentially the same. The exposure time was again 1/100 sec.

PHOTO 15 (Serial No. 176-8) Close-up view of the cylindrical injection nozzle showing injected fluid in contact with downstream side of nozzle (slightly darker area immediately downstream and adjacent to nozzle 1). This condition occured only when the injector velocity was significantly less than the tunnel velocity. In this photo the tunnel velocity is 2.5 fps and the injector velocity is 1.8 fps.

PHOTO 16 (Serial No. 176-58) Conditions similar to those shown in Photo 15 for the cylindrical nozzle also occur for the streamlined nozzle at low injection velocities. Both the tunnel and injector velocities are 2.5 fps.

PHOTO 17 (Serial No. 176-43) Close-up view of the lucite tube used in the vibration tests. The tube, 2 in. I.D. and 6 in. long, is connected to a strain gage dynamometer and installed in the tunnel. A plate over the end of the tube prevented the tube from filling with water.

PHOTO 18 (Serial No. 176-44) Close-up view of the open-end copper tube used in vibration tests. This tube was also 2 in. I.D. and 6 in. long and was installed in the tunnel by the same method used for the lucite tube shown in Photo 17.

PHOTO 1 (Serial No. 176-73) Overall view of tunnel showing the head section and tailwater section. Dyed water is being injected through the streamlined nozzle. Both the tunnel and injector velocities are 5 fps.

PHOTO 2 (Serial No. 176-72) Streamlined injection nozzle formed by fitting a 6 in. long wood housing over a 2 in. I.D. copper tube.

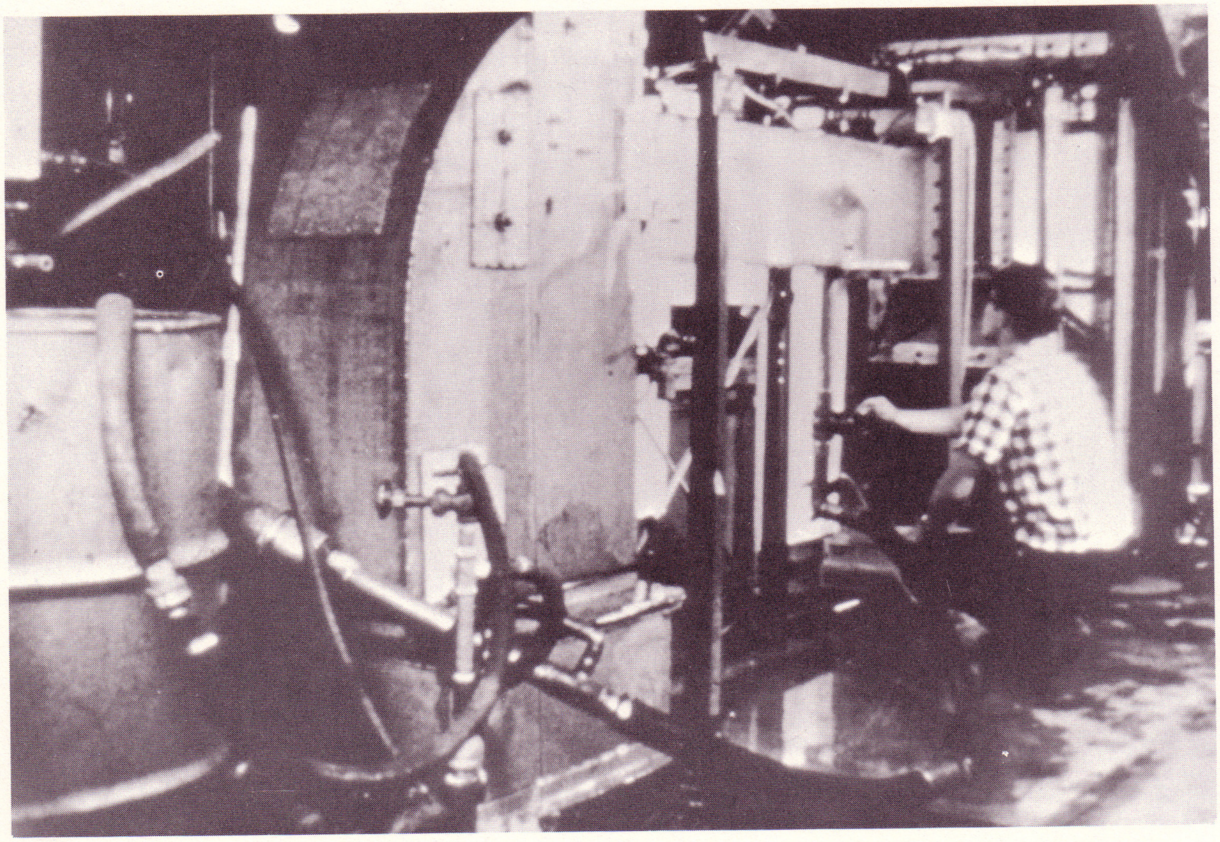

Photo 1

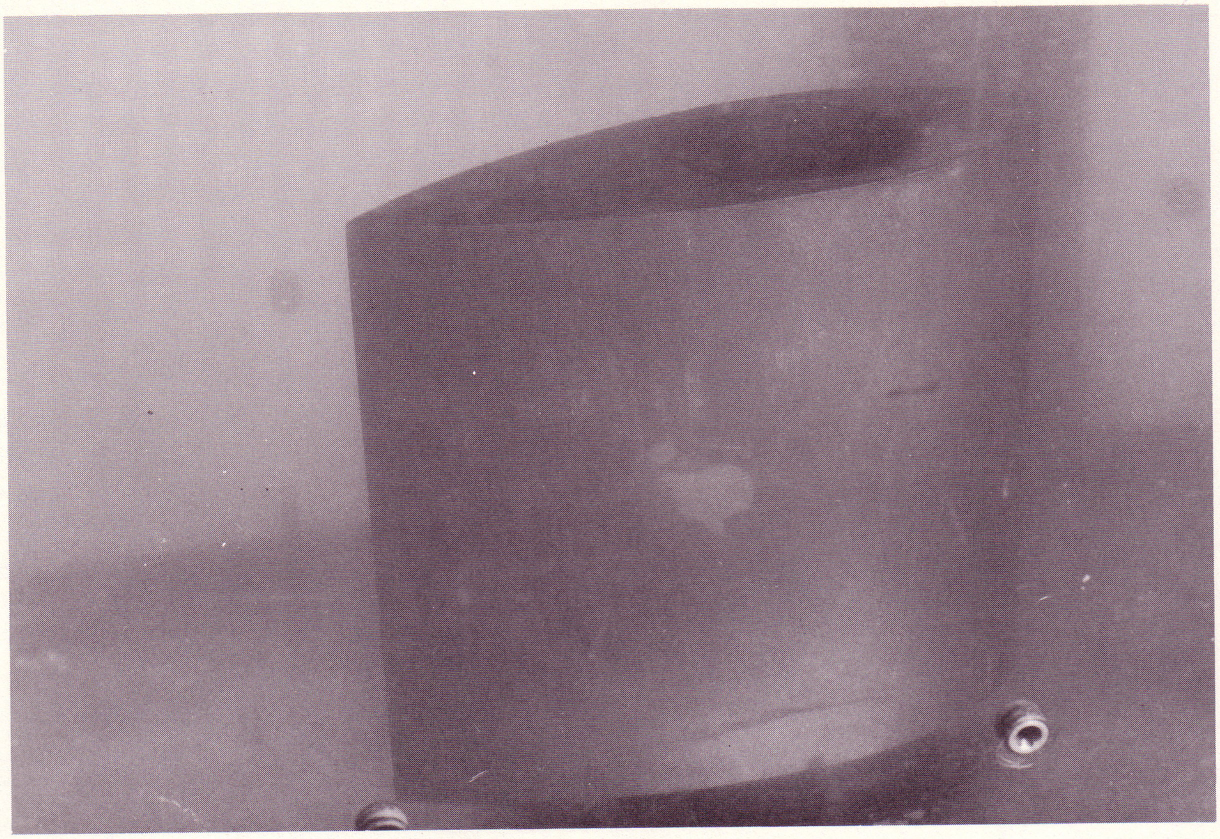

Photo 2

PHOTO 3 (Serial No. 176-45) Overall view of vibration test equipment. Cylindrical copper tube injection nozzle, 2 in. I.D., 6 in. long, is installed in the tunnel (background). The vibrational force and frequency are being recorded on a Sanborn recorder (foreground).

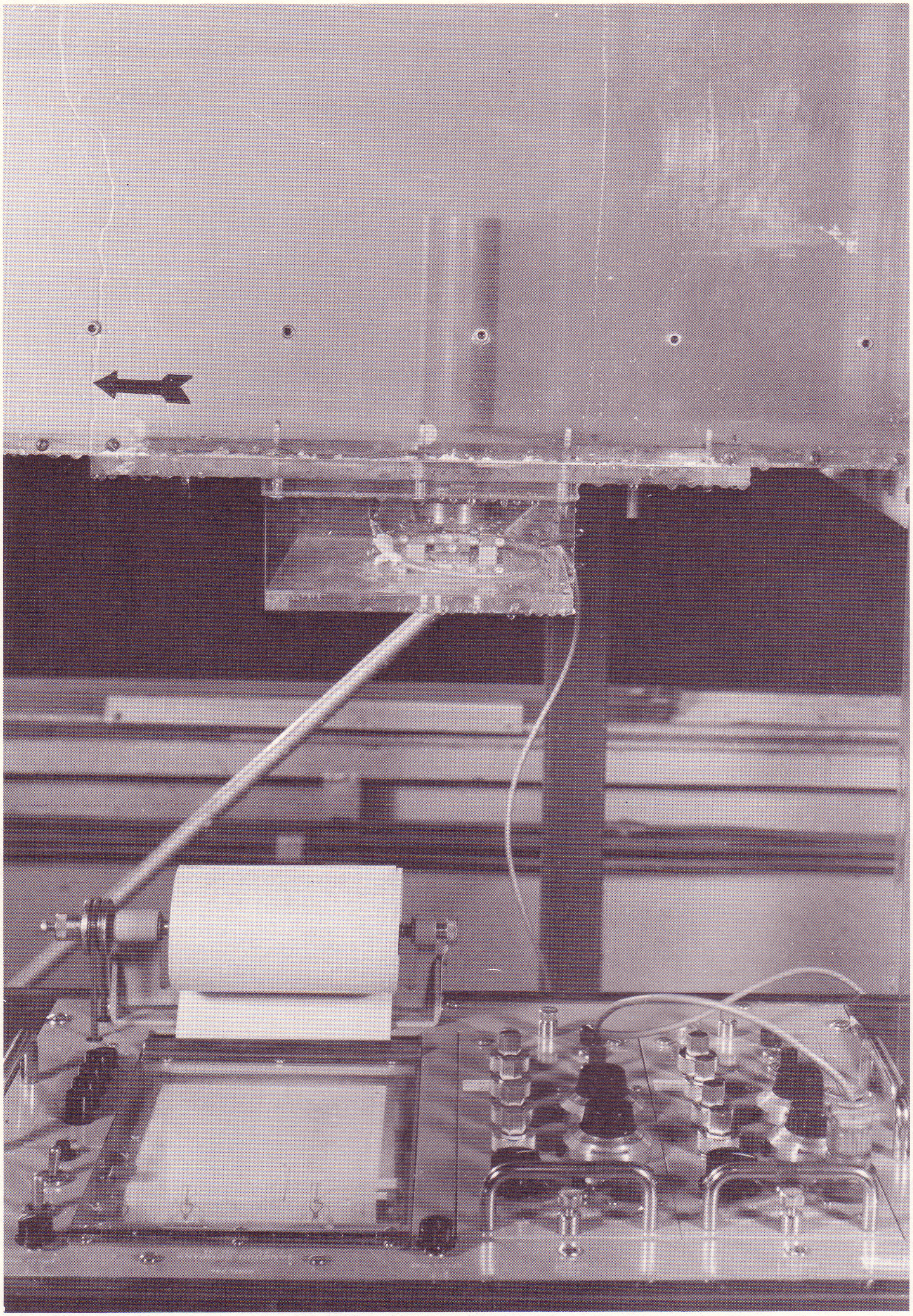

Photo 3

PHOTO 4 (Serial No. 176-41) Close-up view of a portion of the panel board used to control the flow to the injection nozzles, the viewing box adjacent to the point of injection (dyed water is being injected), and the operator titrating a sample taken from the 10 in. diameter pipe.

PHOTO 5 (Serial No. 176-31) Lengthwise view of the 10 in. diameter pipe-line test facility. The manometers used to measure the friction loss and the viewing box adjacent to the injection point are visible in the foreground.

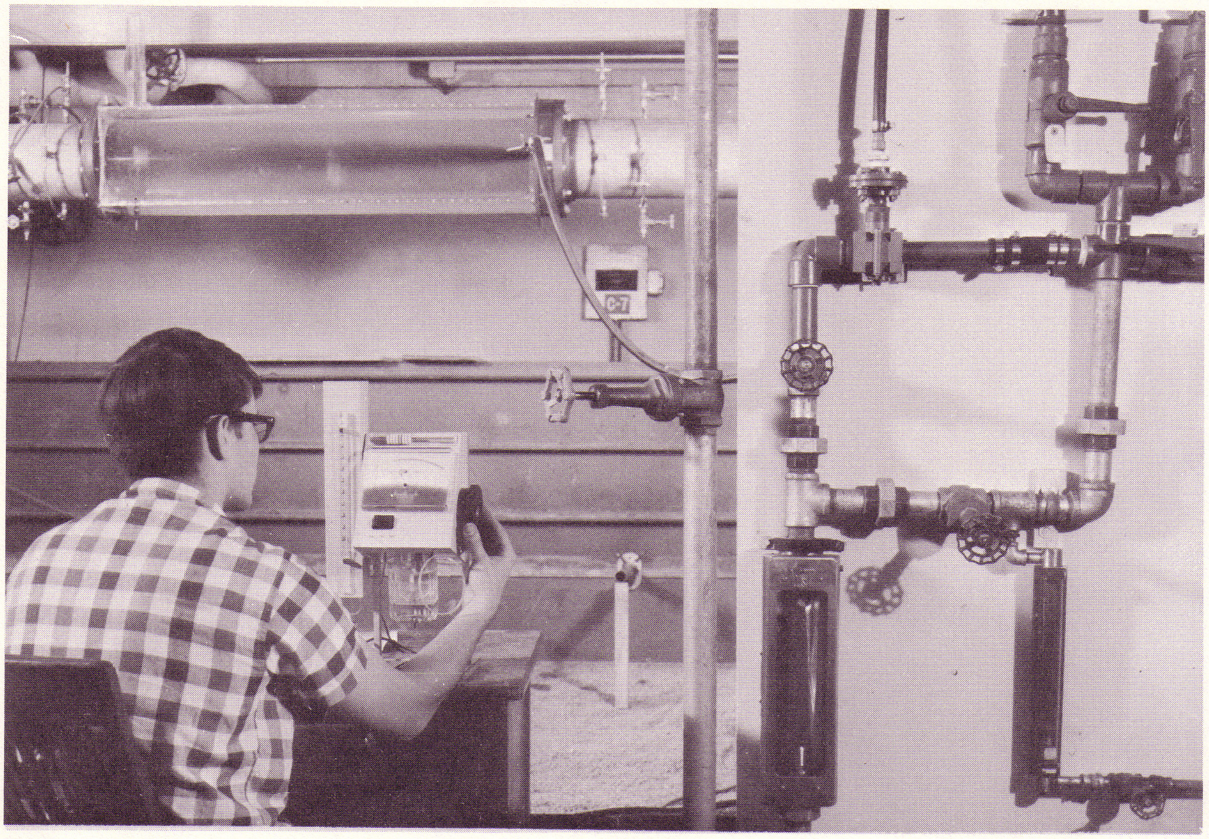

Photo 4

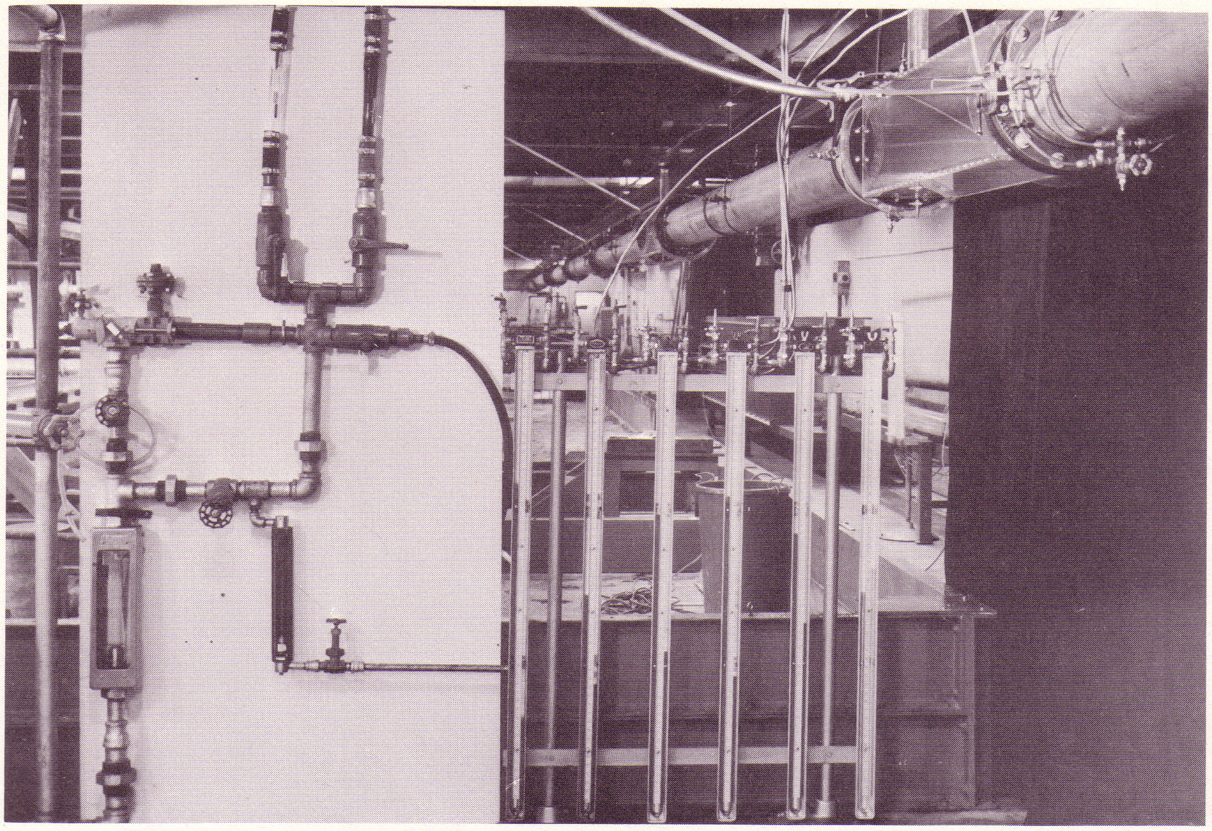

Photo 5

PHOTO 6 (Serial No. 176-7) In Photos 6 through 14 water marked with potassium permanganate is being injected into the water tunnel through a 2 in. I.D., 6 in. long injector nozzle for various flow conditions. In Photo 6 the tunnel velocity is 5 fps and the injector velocity is 1.8 fps. The general dispersion pattern downstream from the injector is shown. A thin film of dyed water (injected fluid) formed on a vertical plane on the downstream side of the nozzle. Exposure time for Photos 6 through 11 is 1/4 sec.

PHOTO 7 (Serial No. 176-9) Tunnel velocity is 5 fps, but the injector velocity has been increased to 3.6 fps. Injected fluid does not collect on the downstream side of the nozzle for these conditions.

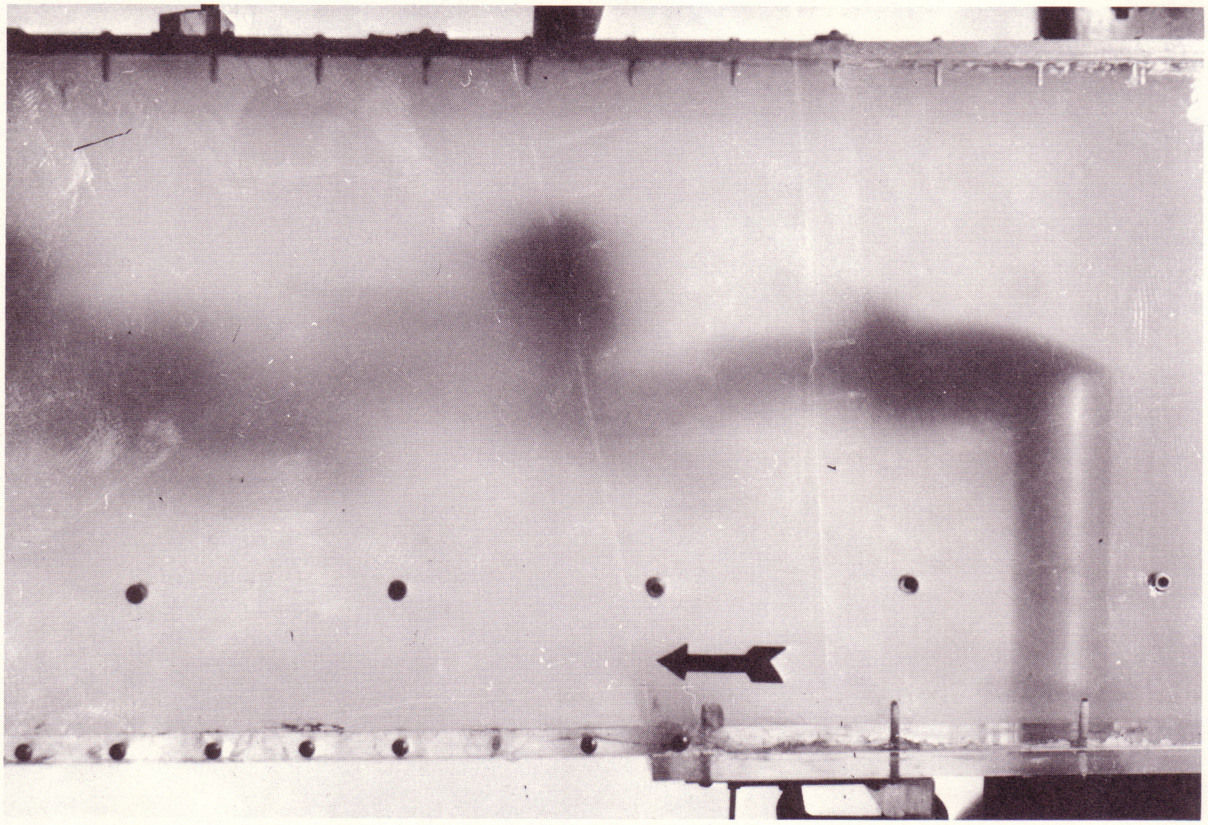

Photo 6

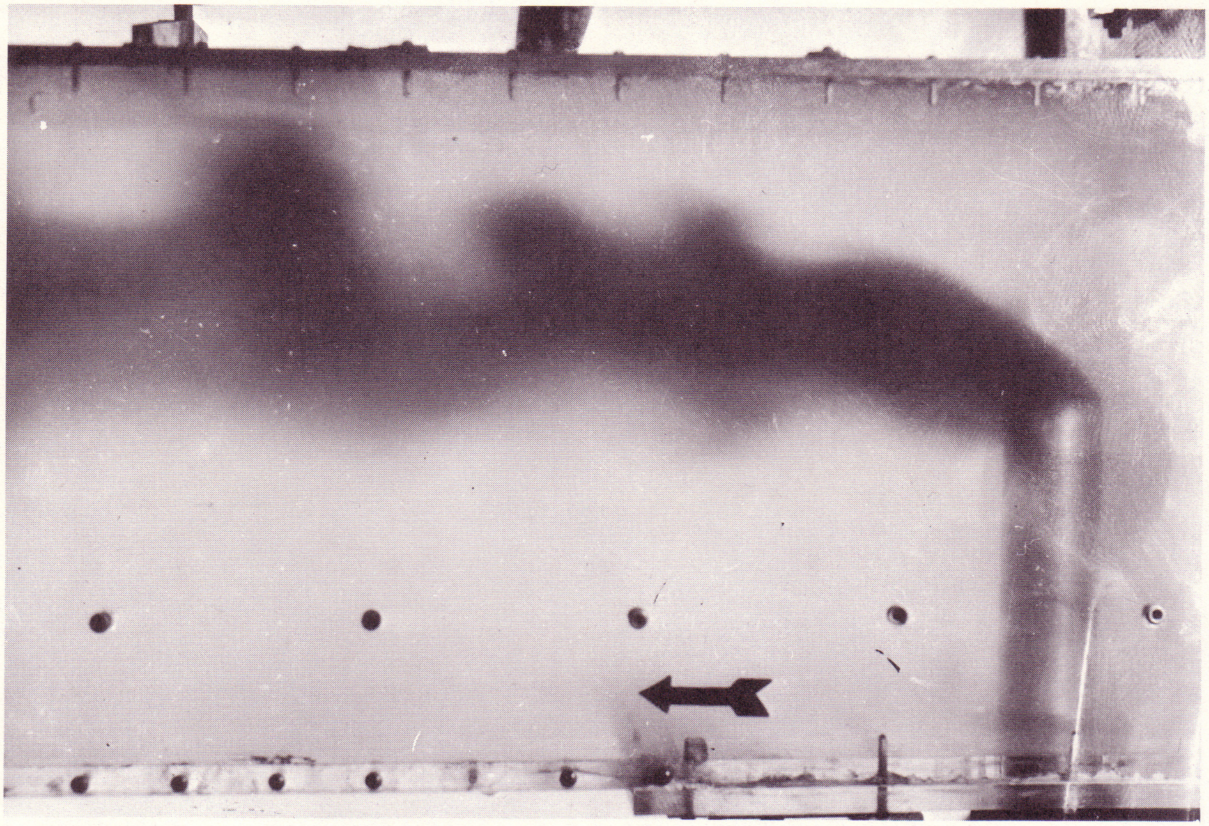

Photo 7

PHOTO 8 (Serial No. 176-11) Injector velocity further increased to 5.4 fps; tunnel velocity maintained at 5 fps. Observe that as the injection velocity is increased from 1.8 to 5.4 fps (Photos 6, 7, and 8), the injected fluid approaches more closely the top boundary of the tunnel. Thus, for pipe flow the injected fluid would be thrust away from the pipe wall and further into the center core of the flow, as the injection velocity was increased.

PHOTO 9 (Serial No. 176-13) Tunnel velocity has been increased to 10 fps; injector velocity is 3.6 fps.

Photo 8

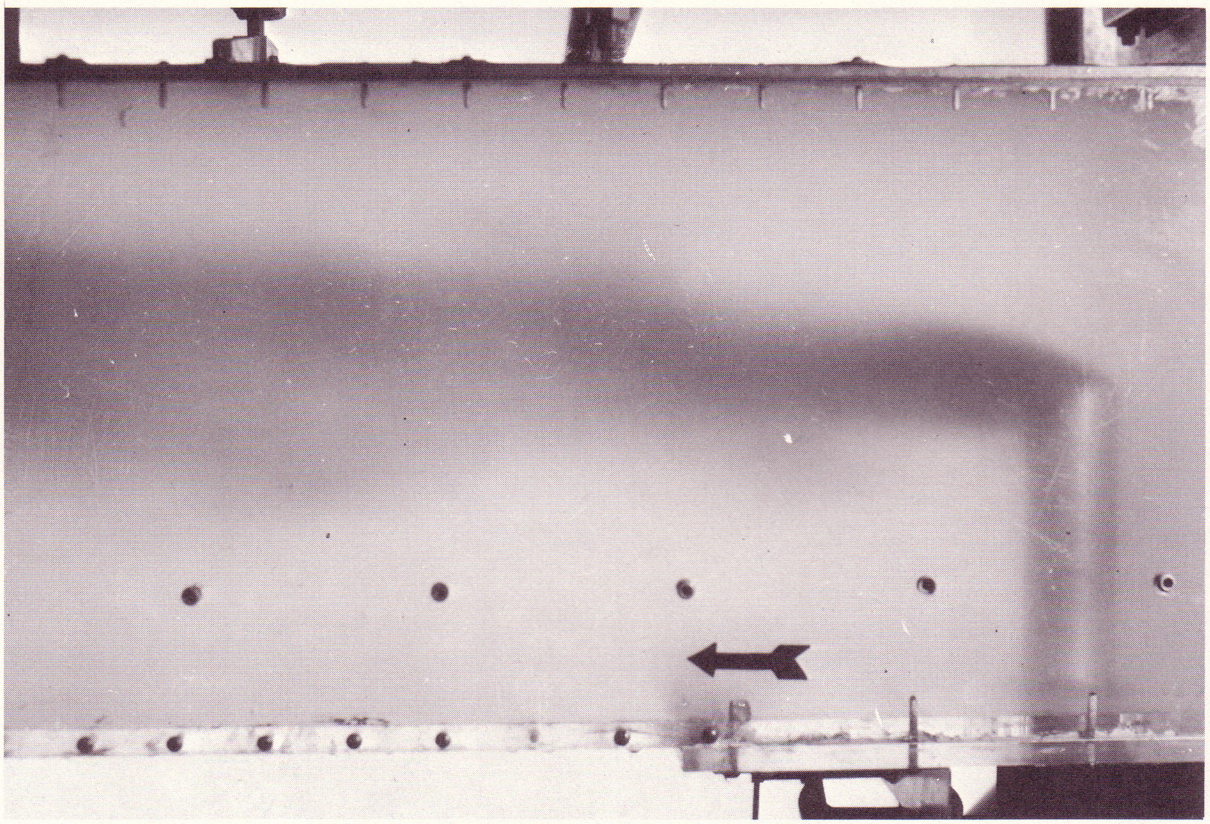

Photo 9

PHOTO 10 (Serial No. 176-15) Tunnel velocity is 10 fps; injector velocity is 7.2 fps.

PHOTO 11 (Serial No. 176-17) Tunnel velocity is 10 fps; injector velocity is 10.8 fps. Comparing Photos 6 and 9, Photos 7 and 10, and Photos 8 and 11, note the similarity of the dispersion pattern when the V_I/V_T ratio is the same.

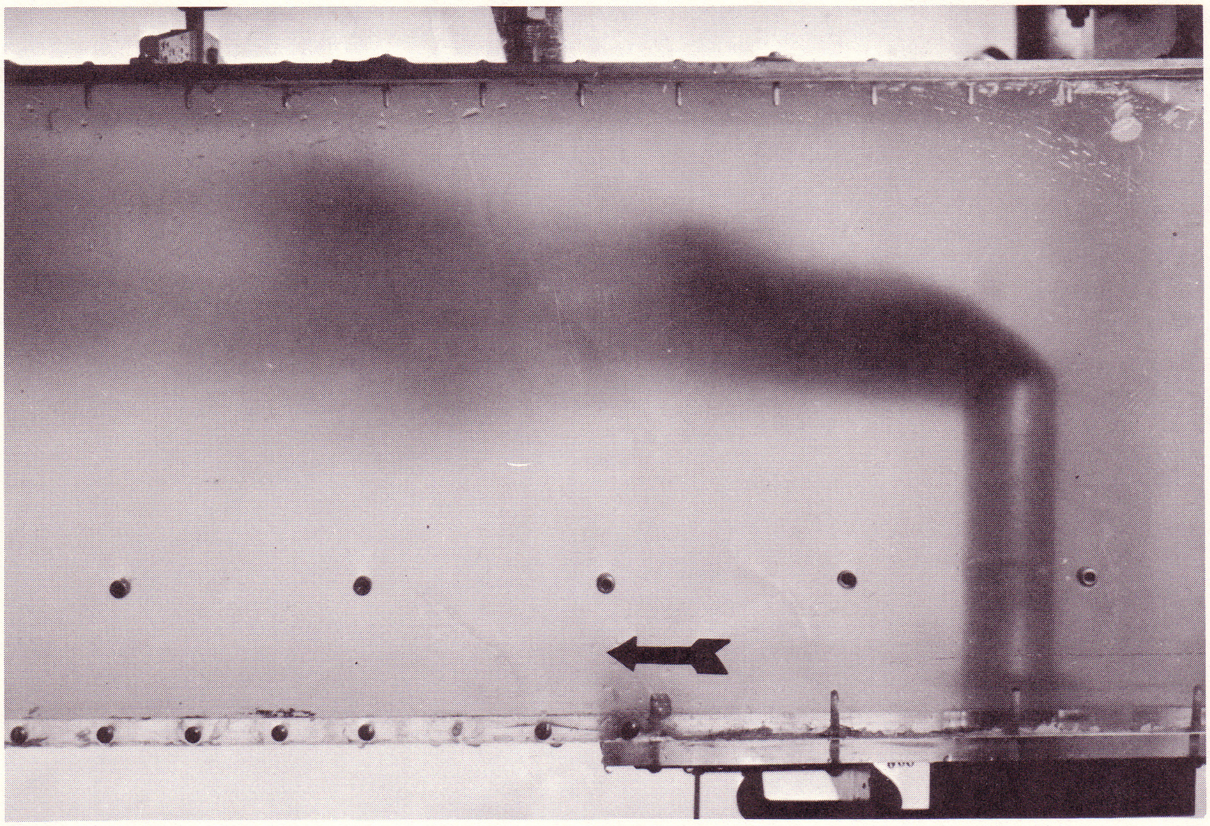

Photo 10

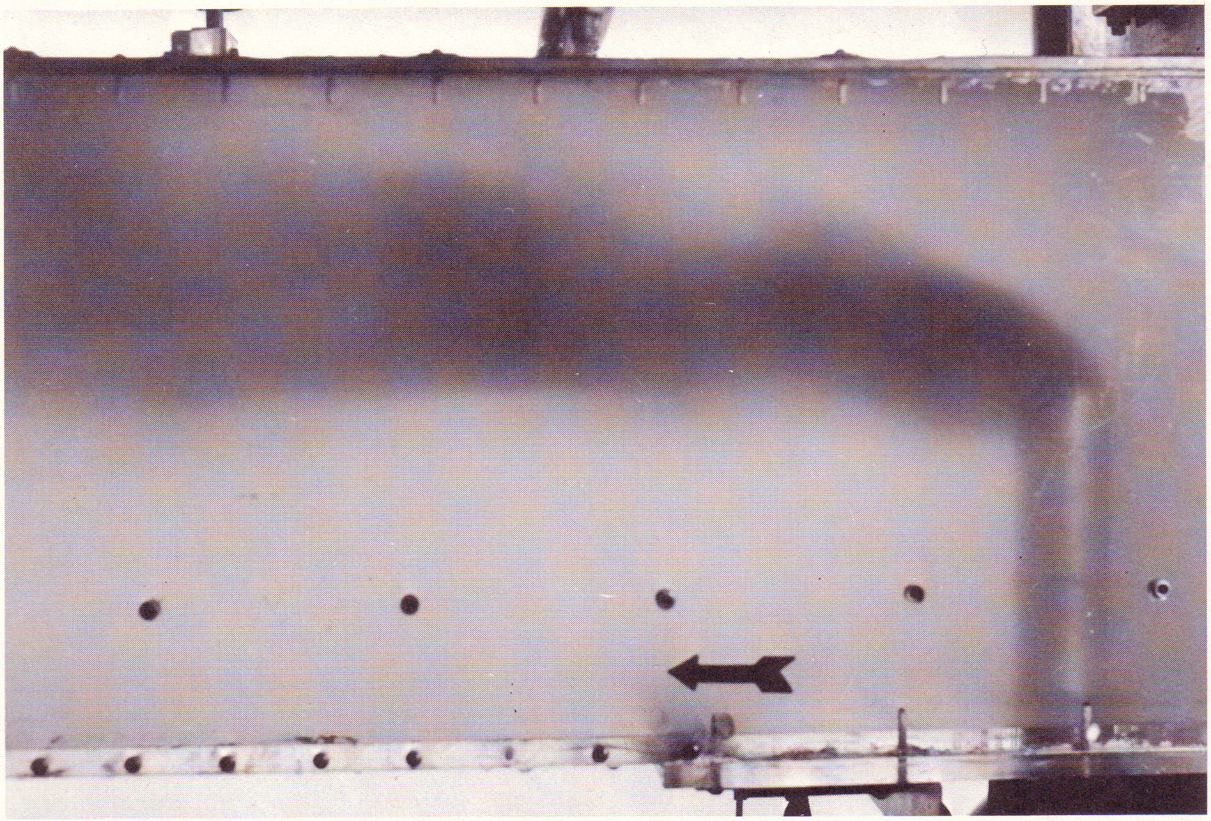

Photo 11

PHOTO 12 (Serial No. 176-49) In this photo and Photo 13 both the tunnel and injector velocities are 5 fps. The photographs were taken with an exposure time of 1/100 sec so that the details of the dispersion pattern for the cylindrical (Photo 12) and streamlined nozzle (Photo 13) could be compared. Each picture shows the dispersion pattern within the first 3 ft downstream of the injection point. Note the similarity of the dispersion patterns.

PHOTO 13 (Serial No. 176-52) Dispersion pattern for streamlined injection nozzle. Tunnel and injection velocities are 5 fps.

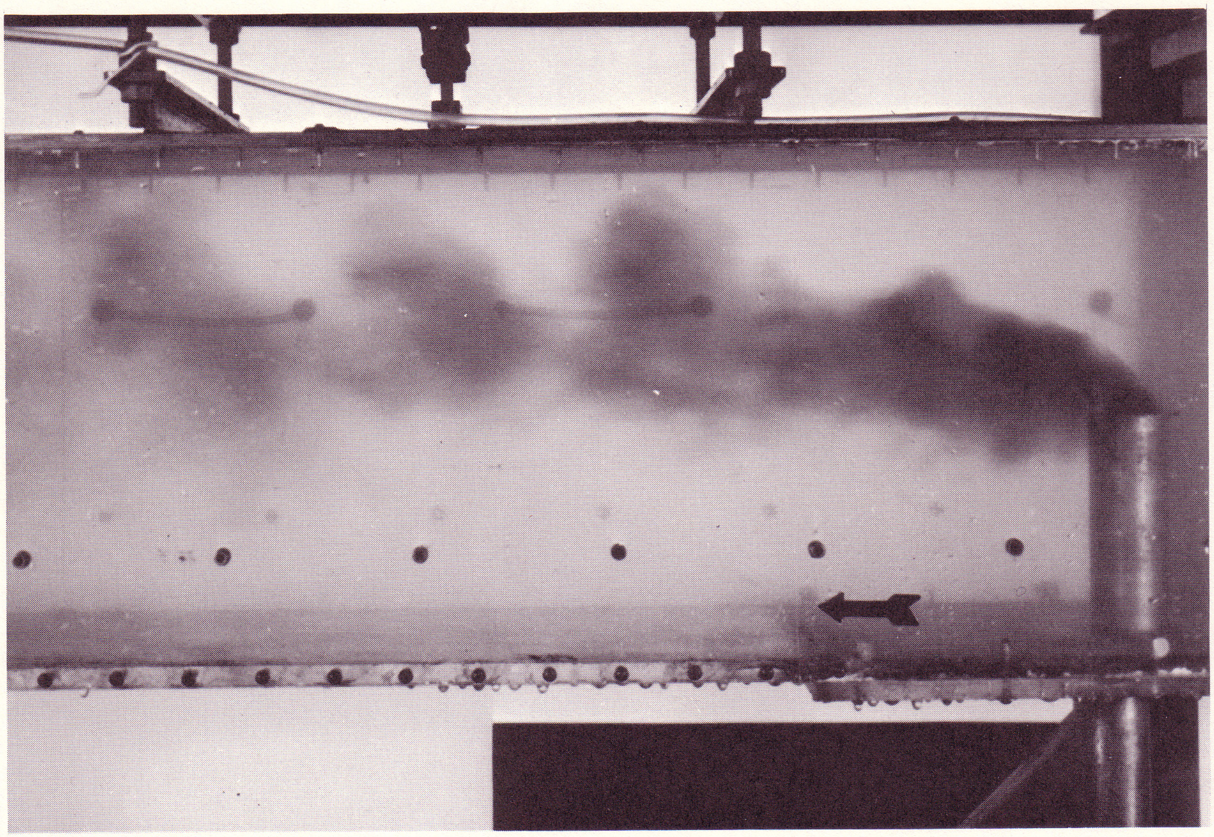

Photo 12

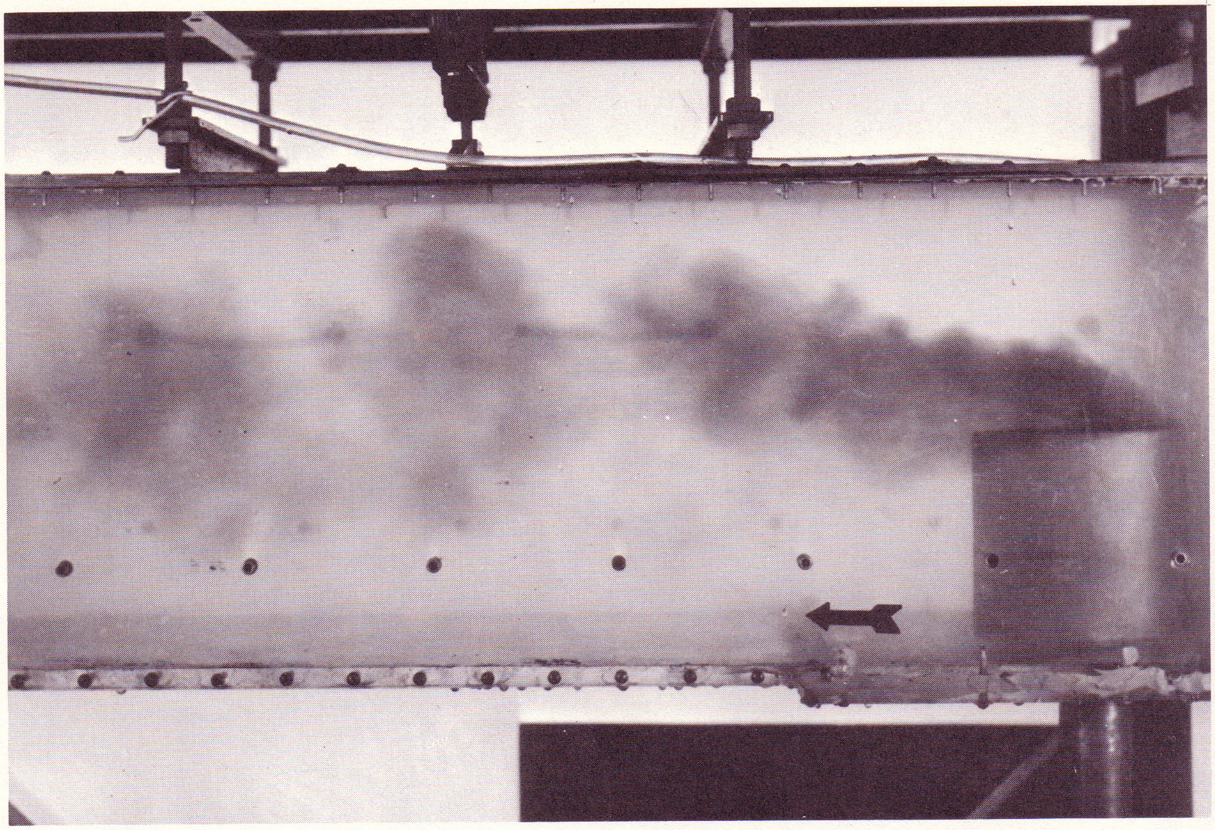

Photo 13

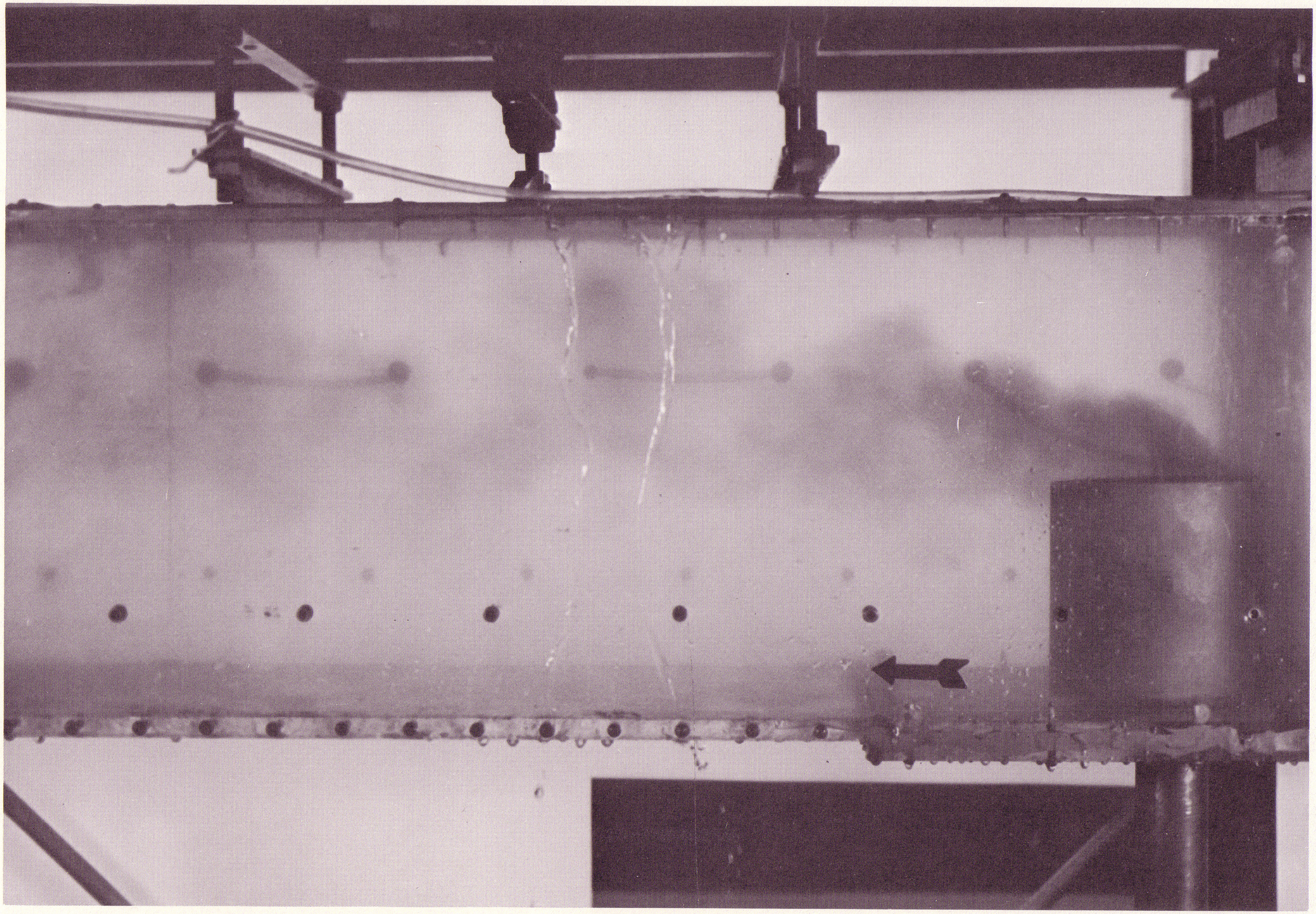

Photo 14

PHOTO 15 (Serial No. 176-8) Close-up view of the cylindrical injection nozzle showing injected fluid in contact with downstream side of nozzle (slightly darker area immediately downstream and adjacent to nozzle 1). This condition occurred only when the injector velocity was significantly less than the tunnel velocity. In this photo the tunnel velocity is 2.5 fps and the injector velocity is 1.8 fps.

PHOTO 16 (Serial No. 176-58) Conditions similar to those shown in Photo 15 for the cylindrical nozzle also occur for the streamlined nozzle at low injection velocities. Both the tunnel and injector velocities are 2.5 fps.

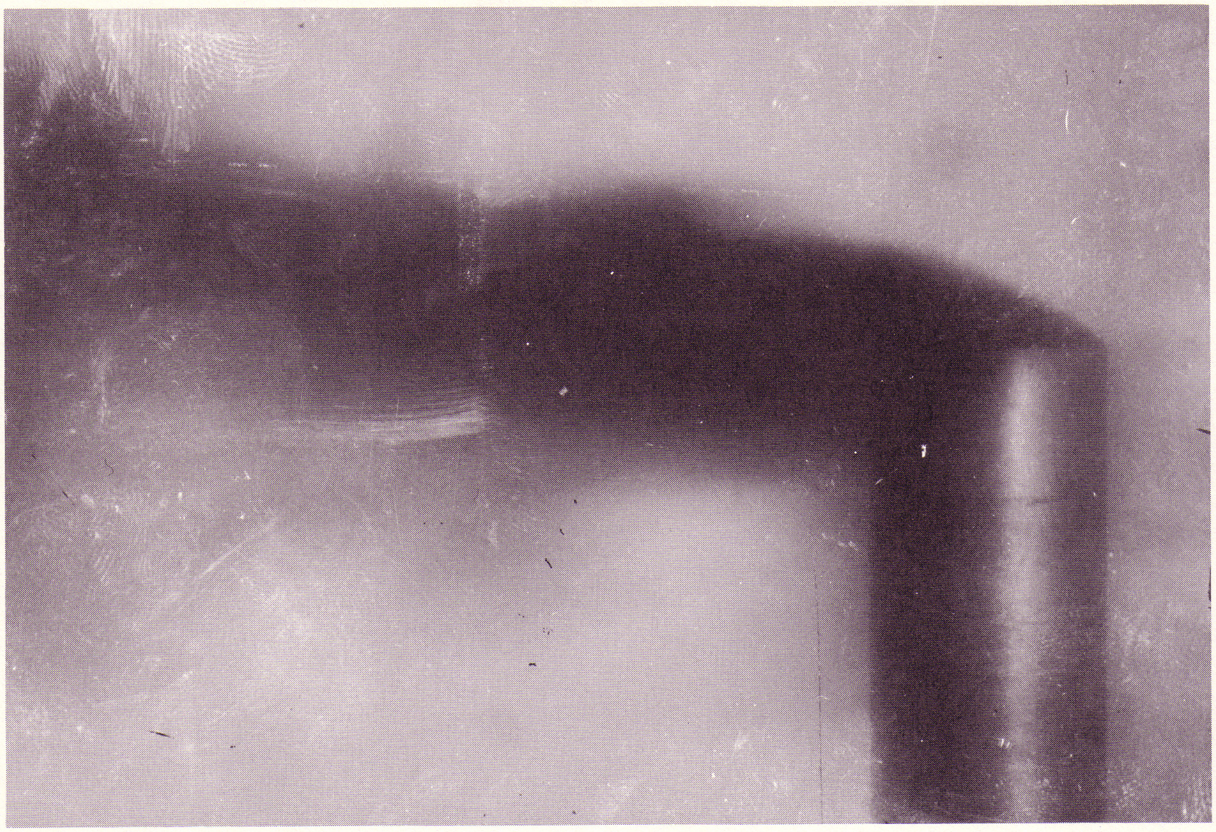

Photo 15

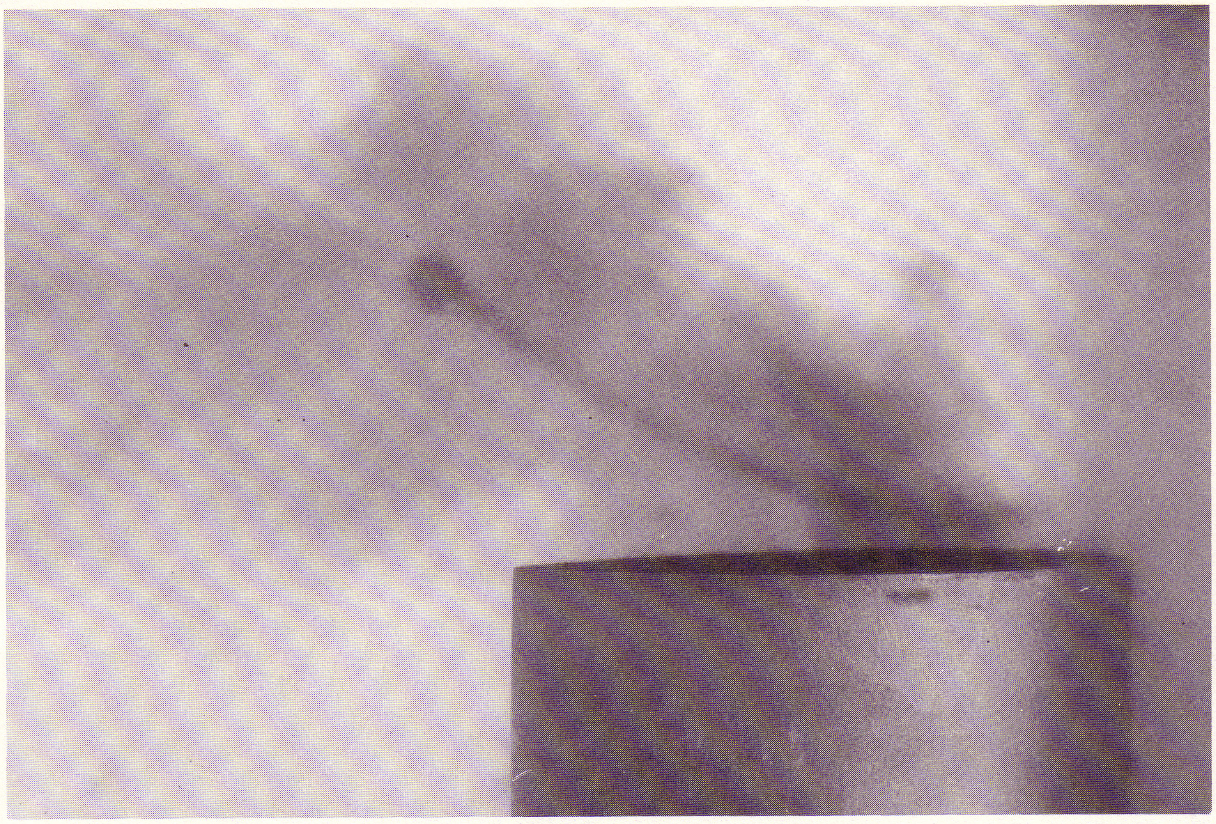

Photo 16

PHOTO 17 (Serial No. 176-43) Close-up view of the lucite tube used in the vibration tests. The tube, 2 in. I.D. and 6 in. long, is connected to a strain gage dynamometer and installed in the tunnel. A plate over the end of the tube prevented the tube from filling with water.

PHOTO 18 (Serial No. 176-44) Close-up view of the open-end copper tube used in vibration tests. This tube was also 2 in. I.D. and 6 in. long and was installed in the tunnel by the same method used for the lucite tube shown in Photo 17.

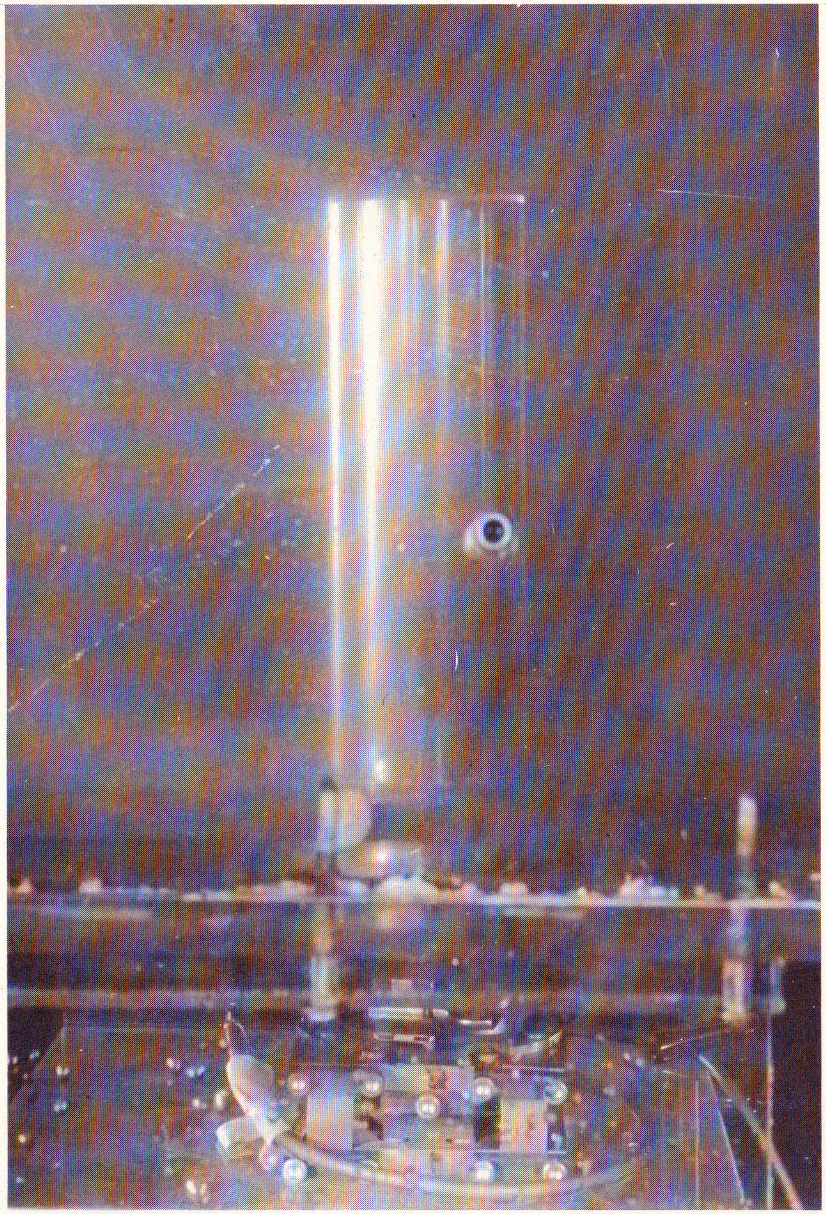

Photo 17

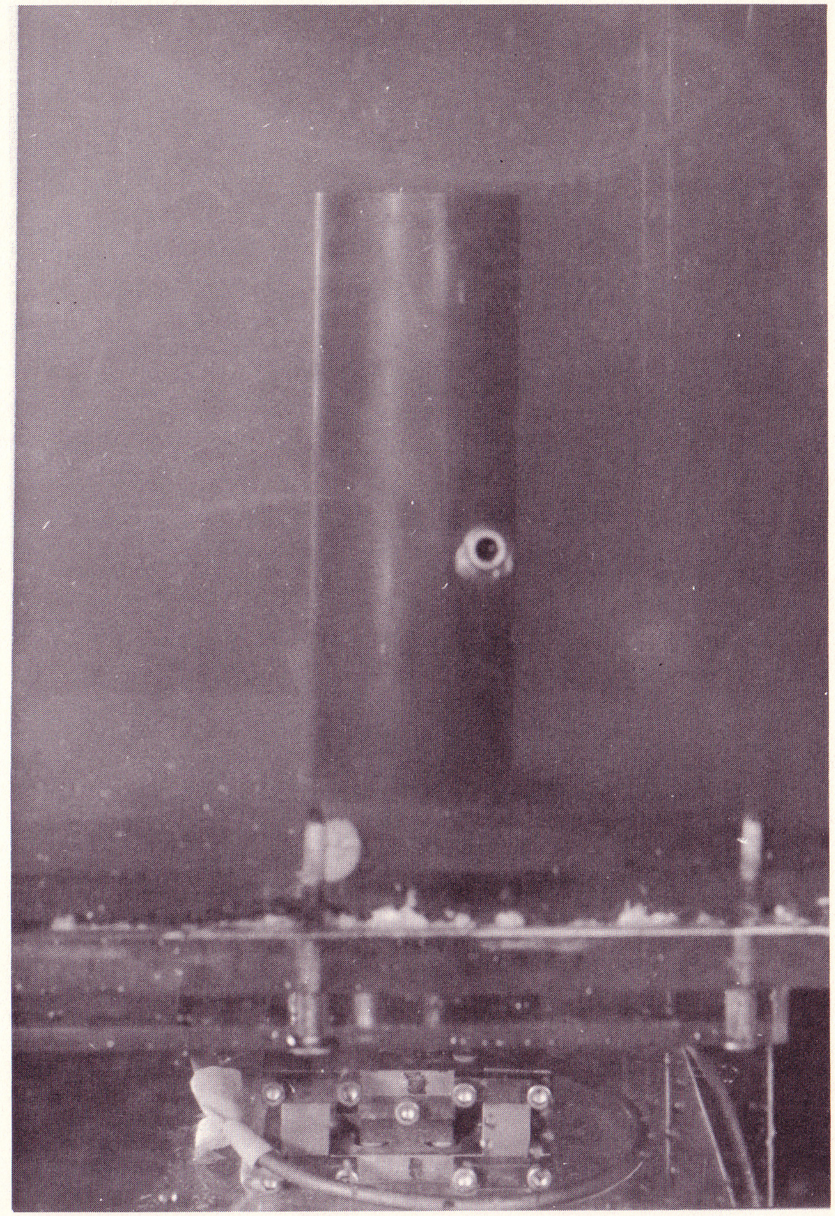

Photo 18

LIST OF FIGURES

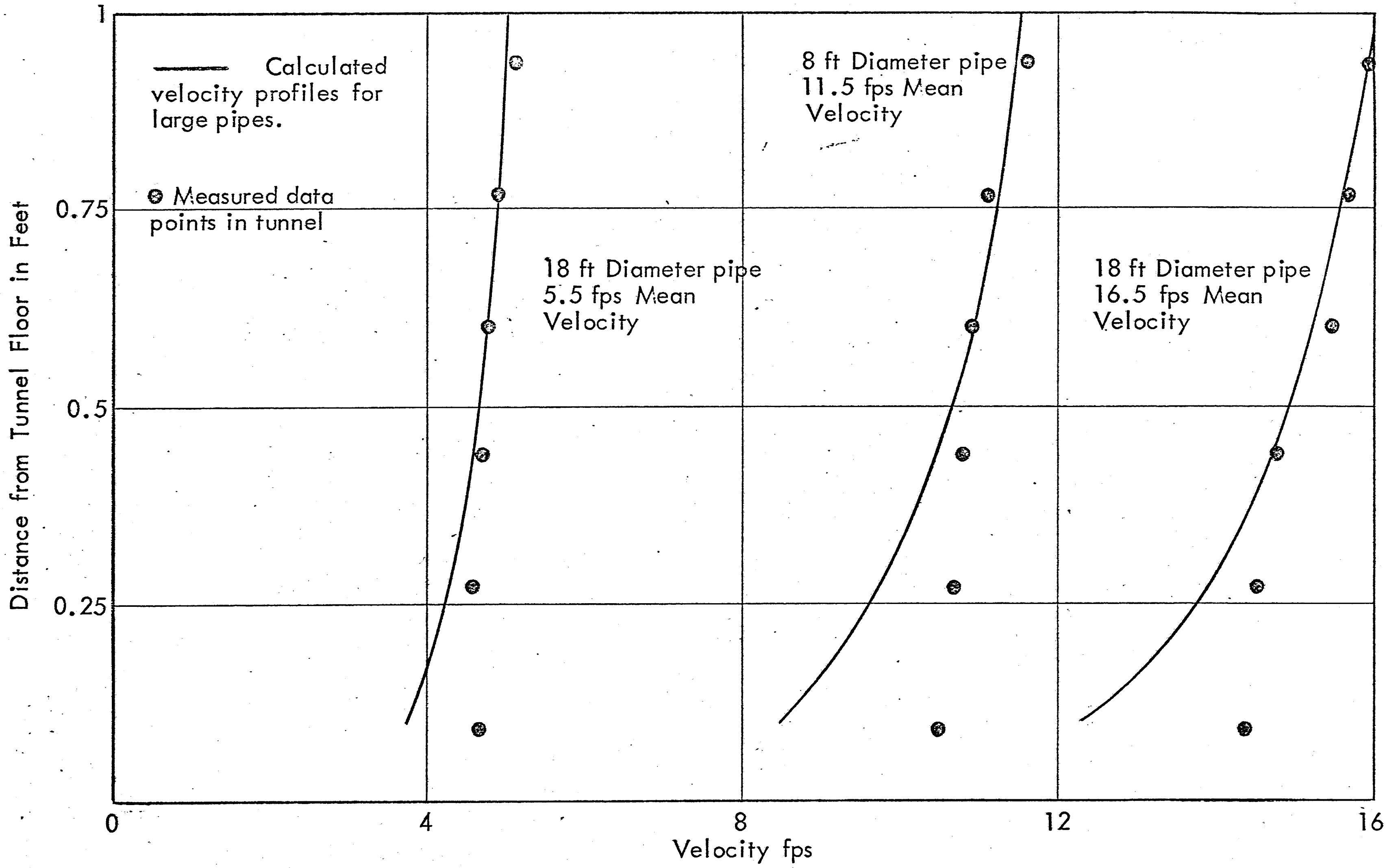

Fig. 1 - Velocity Profiles in Nozzle Test Apparatus

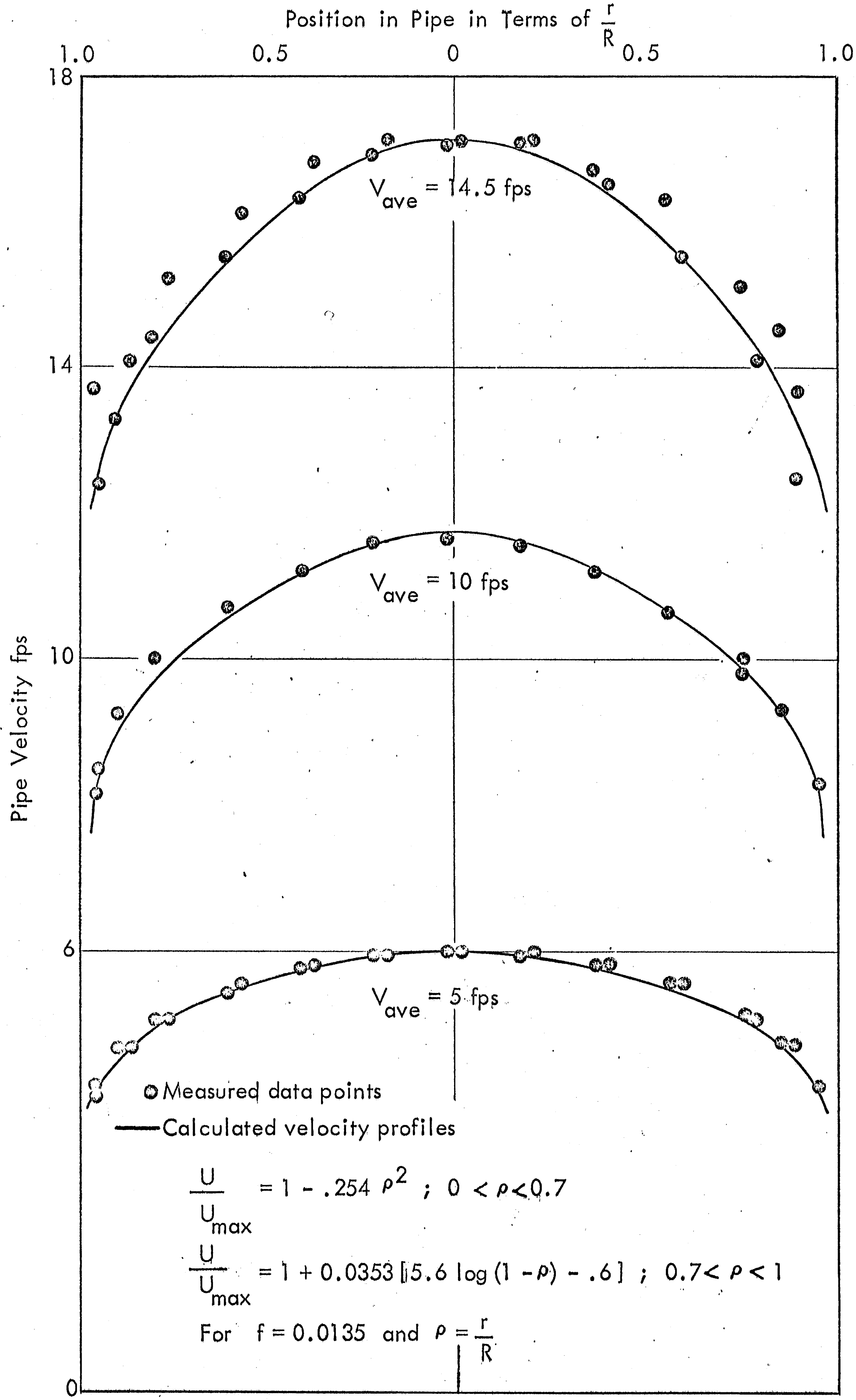

Fig. 2 - Velocity Profiles for 10 inch Diameter Pipe

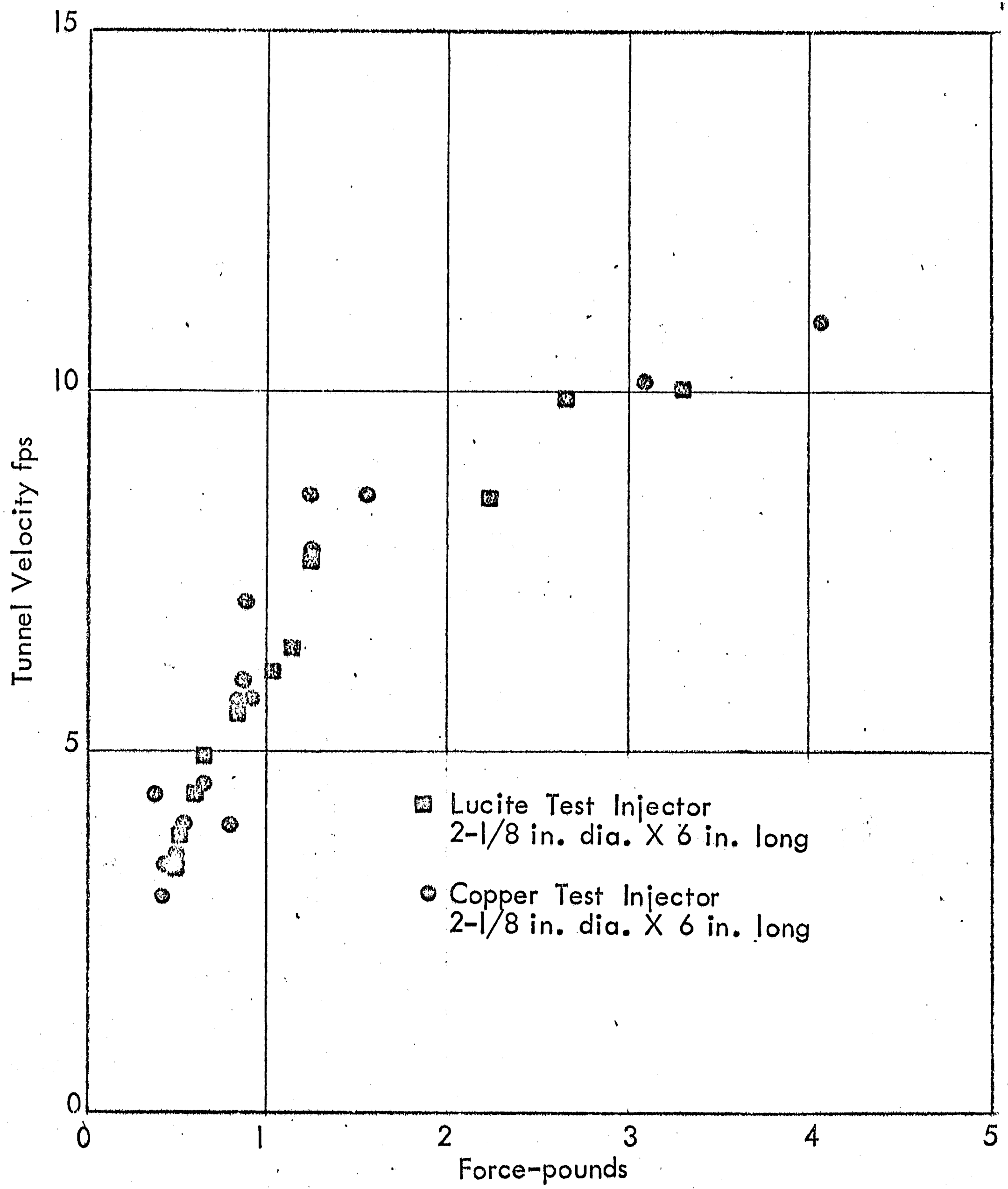

Fig. 3 - Vibration Force Acting on Injection Nozzle as a Function of Tunnel Velocity

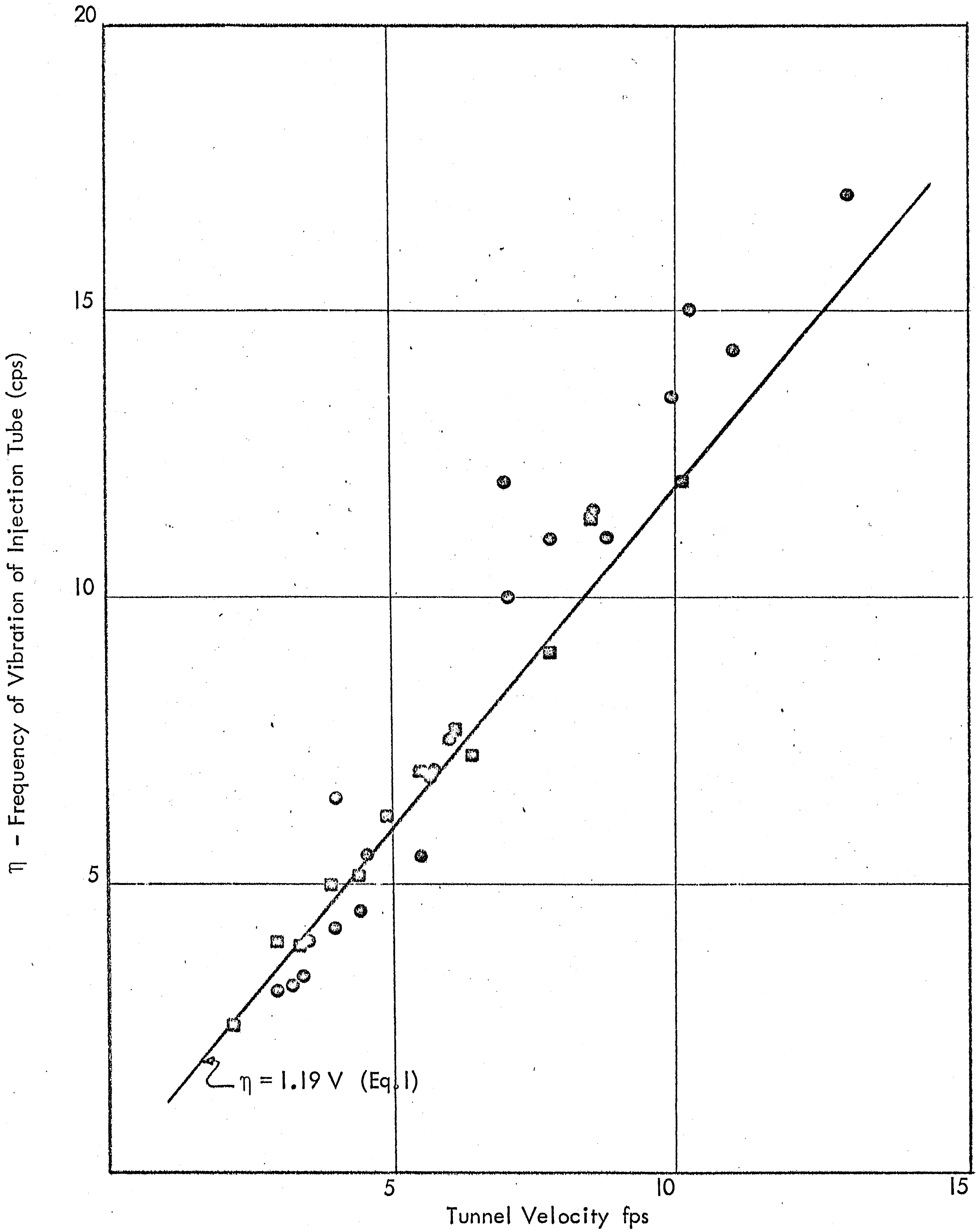

Fig. 4 - Measured Vibrational Frequency as a Function of Tunnel Velocity

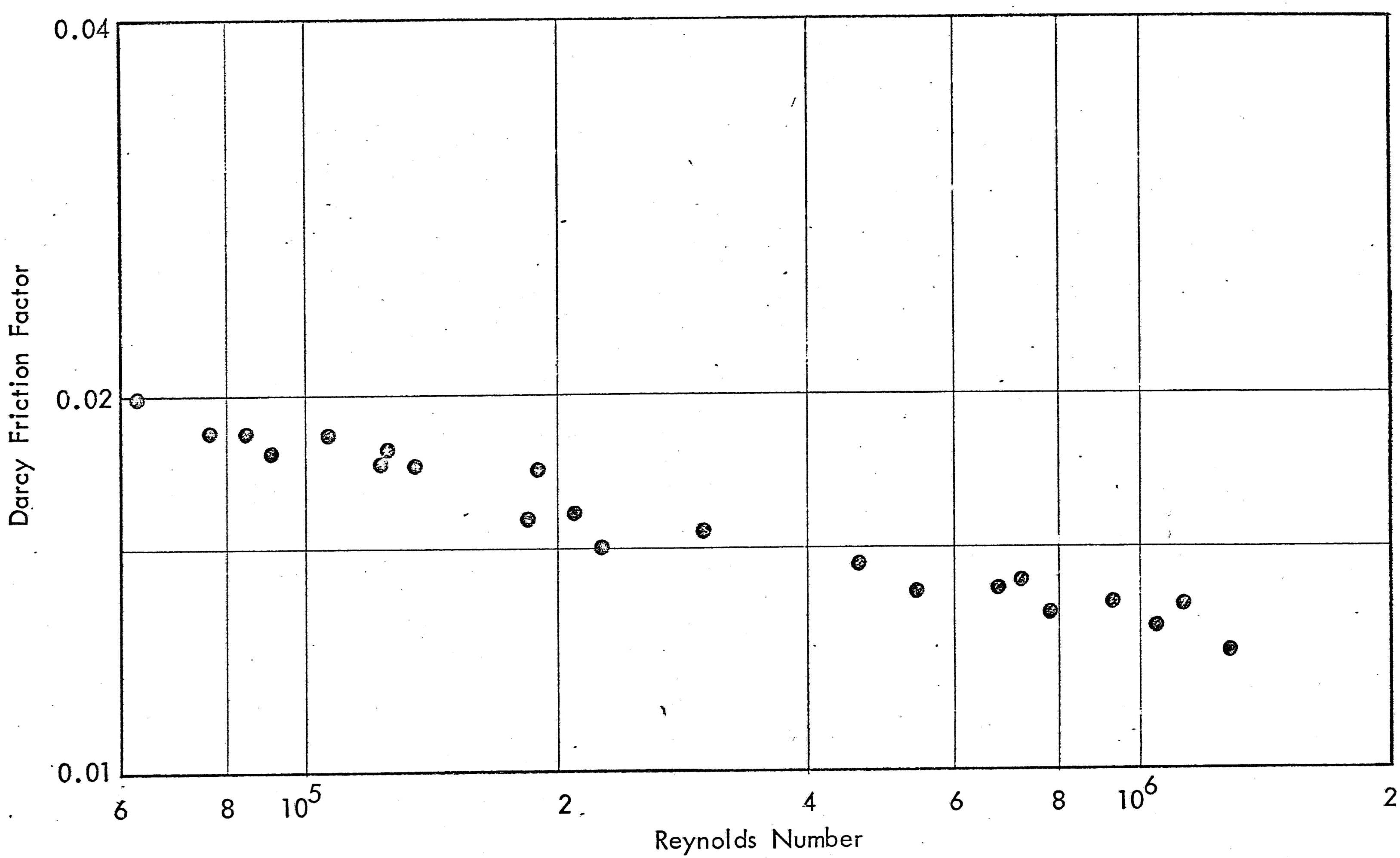

Fig. 5 - Friction Factor as a Function of Reynolds Number for 10 inch Diameter Pipe

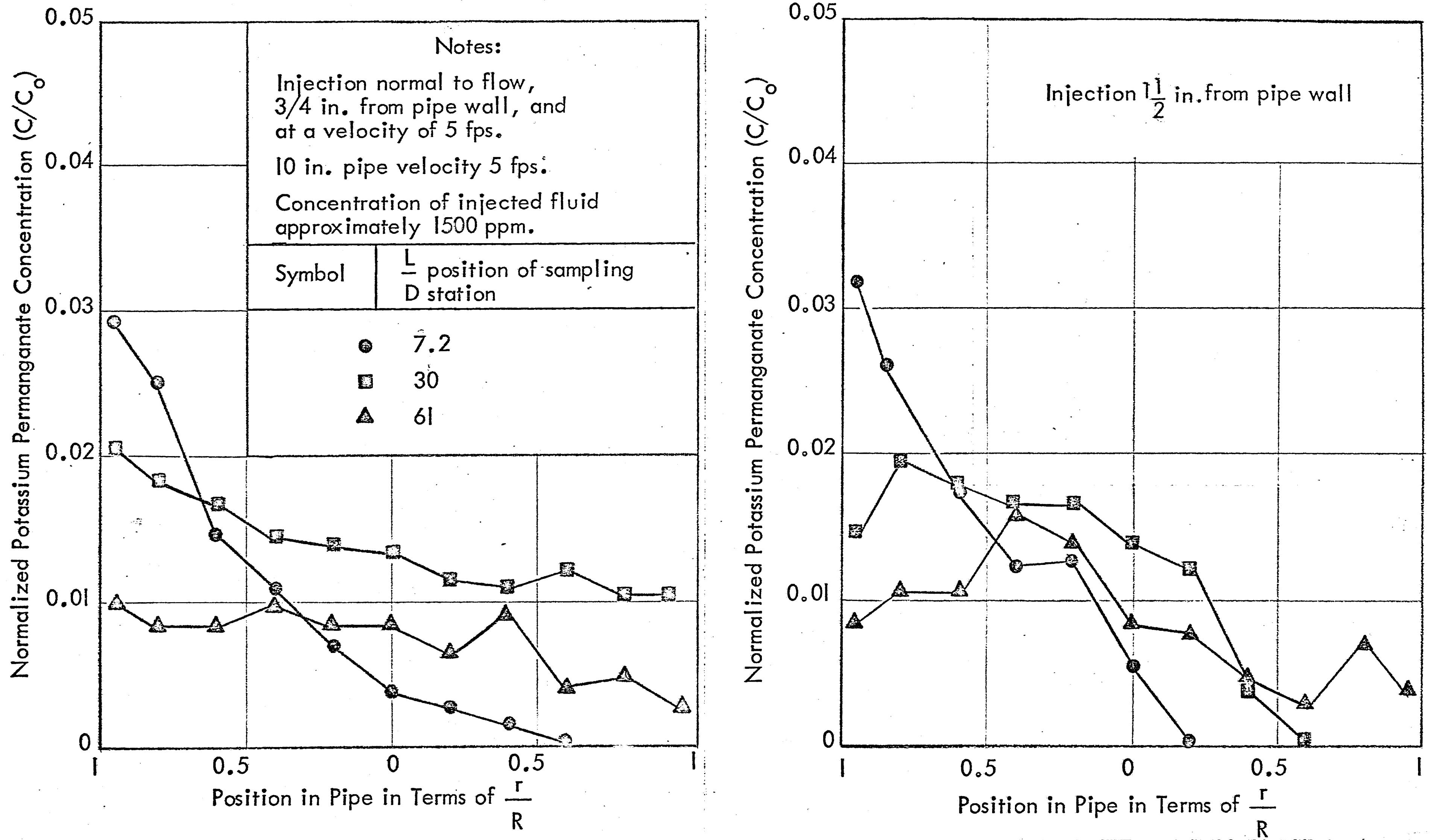

Fig. 6 – Concentration Profiles Across the Horizontal Diameter at Various $\frac{L}{D}$ Values Downstream from the Injection Point; Injection Potassium Permanganate Solution through one Injector.

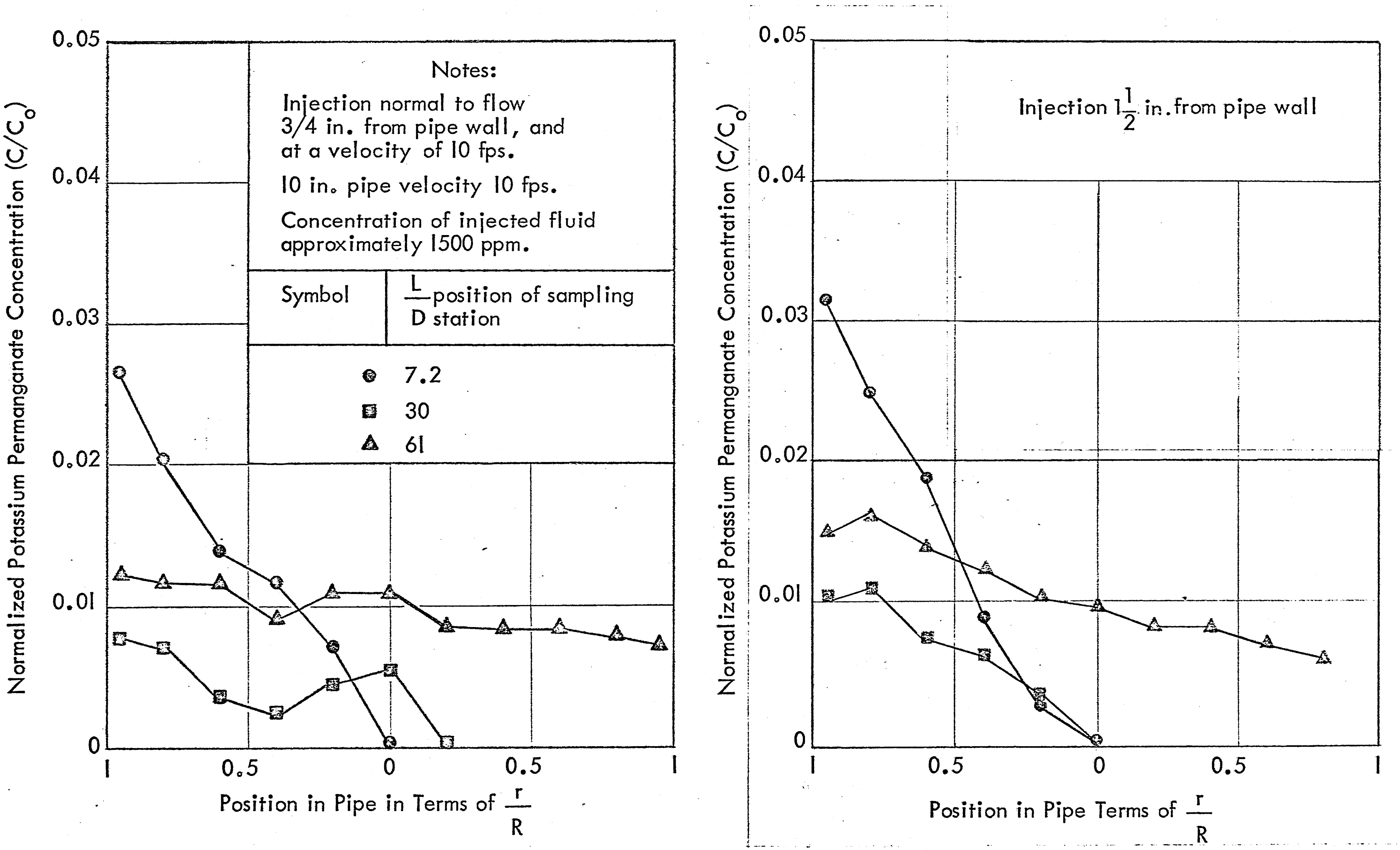

Fig. 7 – Concentration Profiles Across the Horizontal Diameter at Various $\frac{L}{D}$ Values Downstream from the Injection Point; Injection Potassium Permanganate Solution through one Injector.

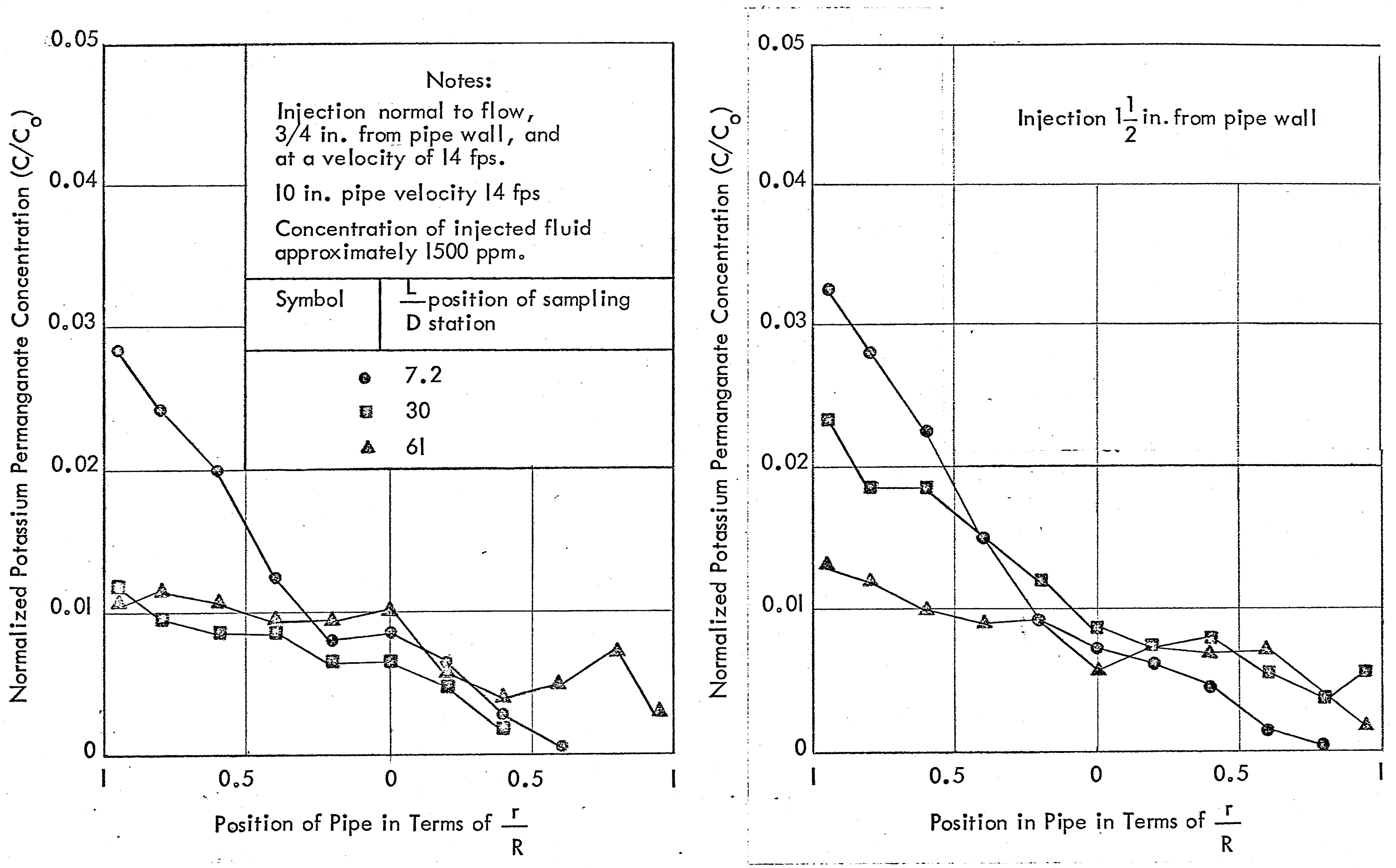

Fig. 8 - Concentration Profiles Across the Horizontal Diameter at Various $\frac{L}{D}$ Values Downstream from the Injection Point; Injection Potassium Permanganate Solution through one Injector.

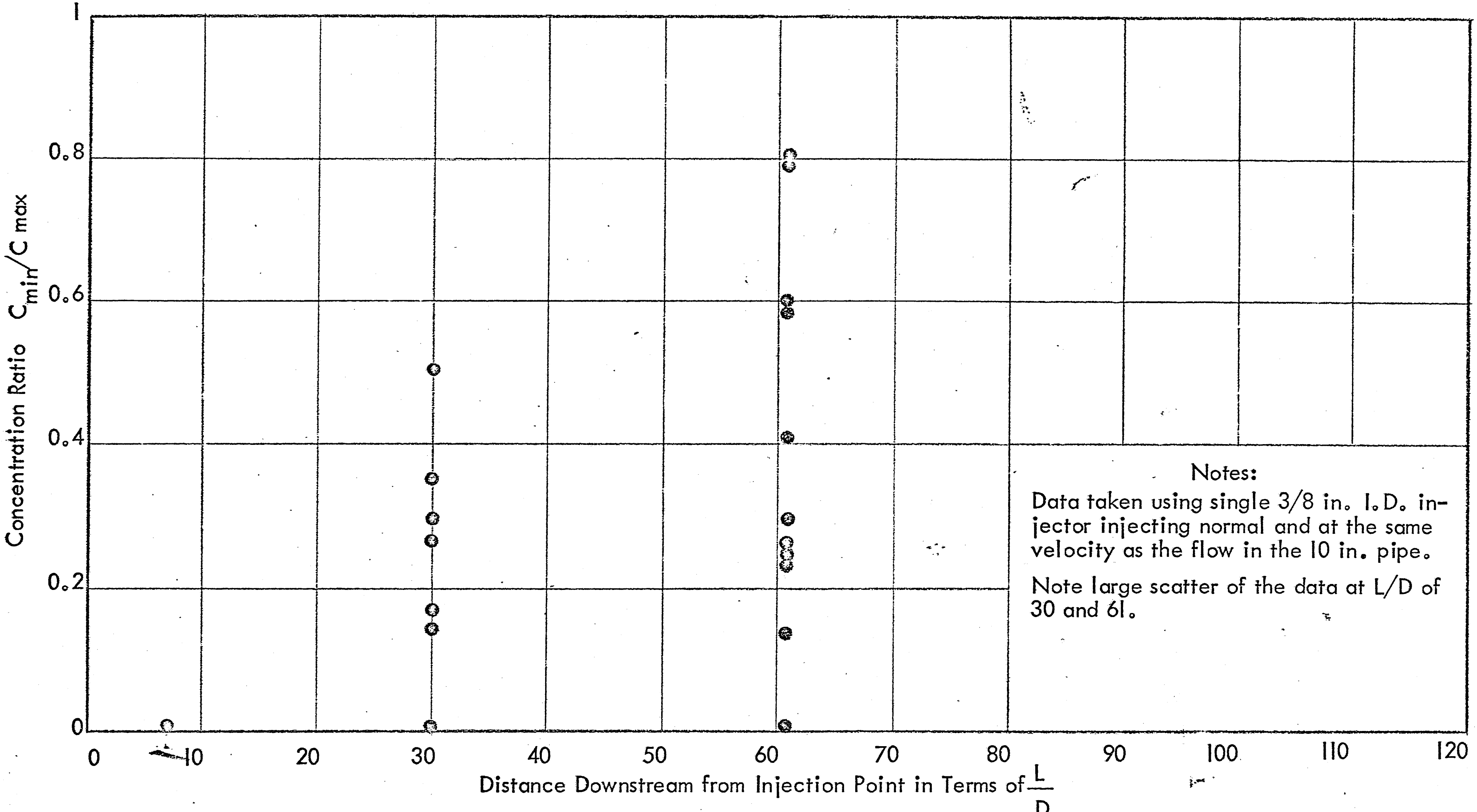

Fig. 9 - C min/C max Ratios at Various $\frac{L}{D}$ Values for the Injection of Potassium Permanganate Solution

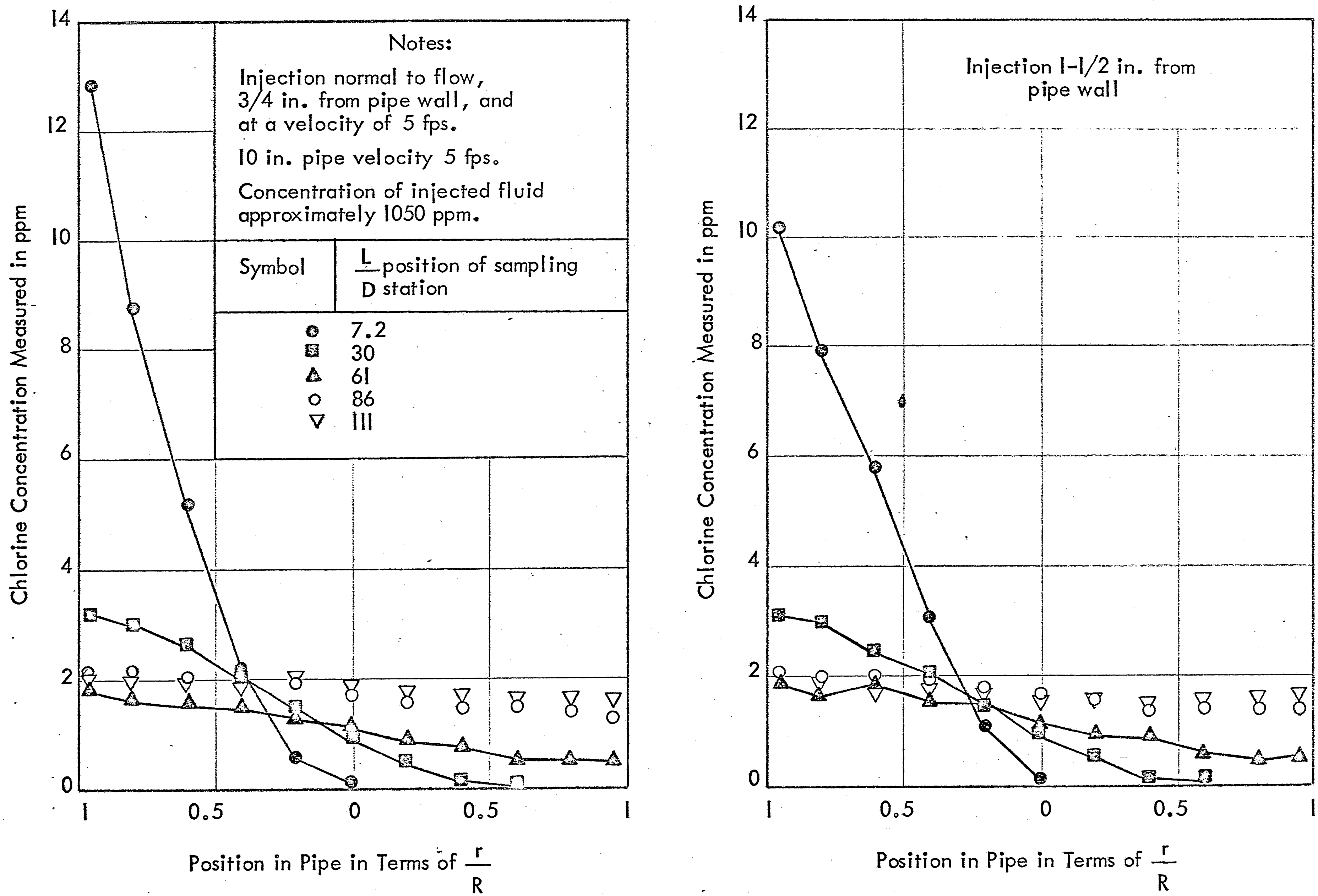

Fig. 10- Concentration Profiles Across the Horizontal Diameter at Various $\frac{L}{D}$ Values Downstream from the Injection Point using one Injector

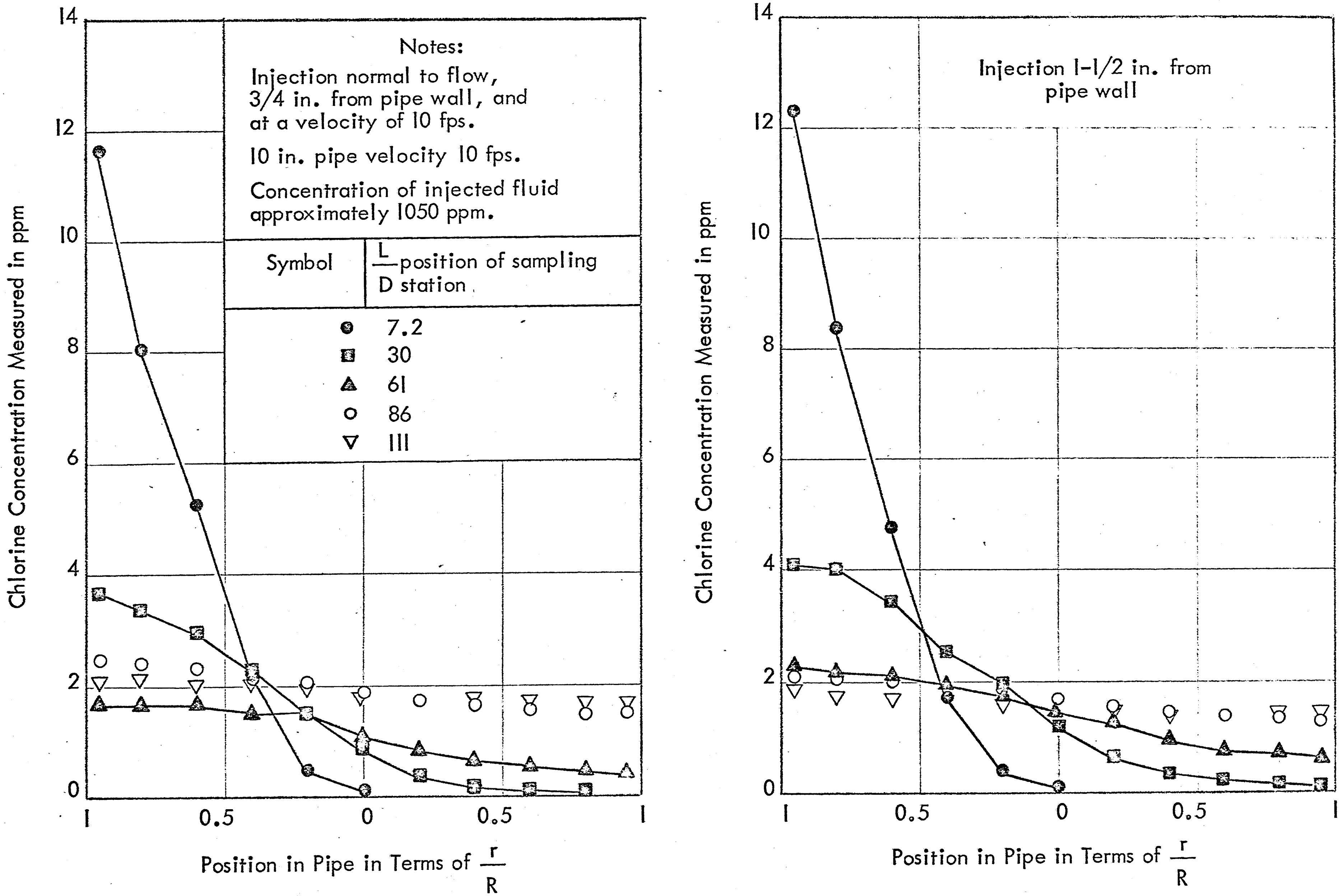

Fig. 11 – Concentration Profiles Across the Horizontal Diameter at Various $\frac{L}{D}$ Values Downstream from the Injection Point using one Injector

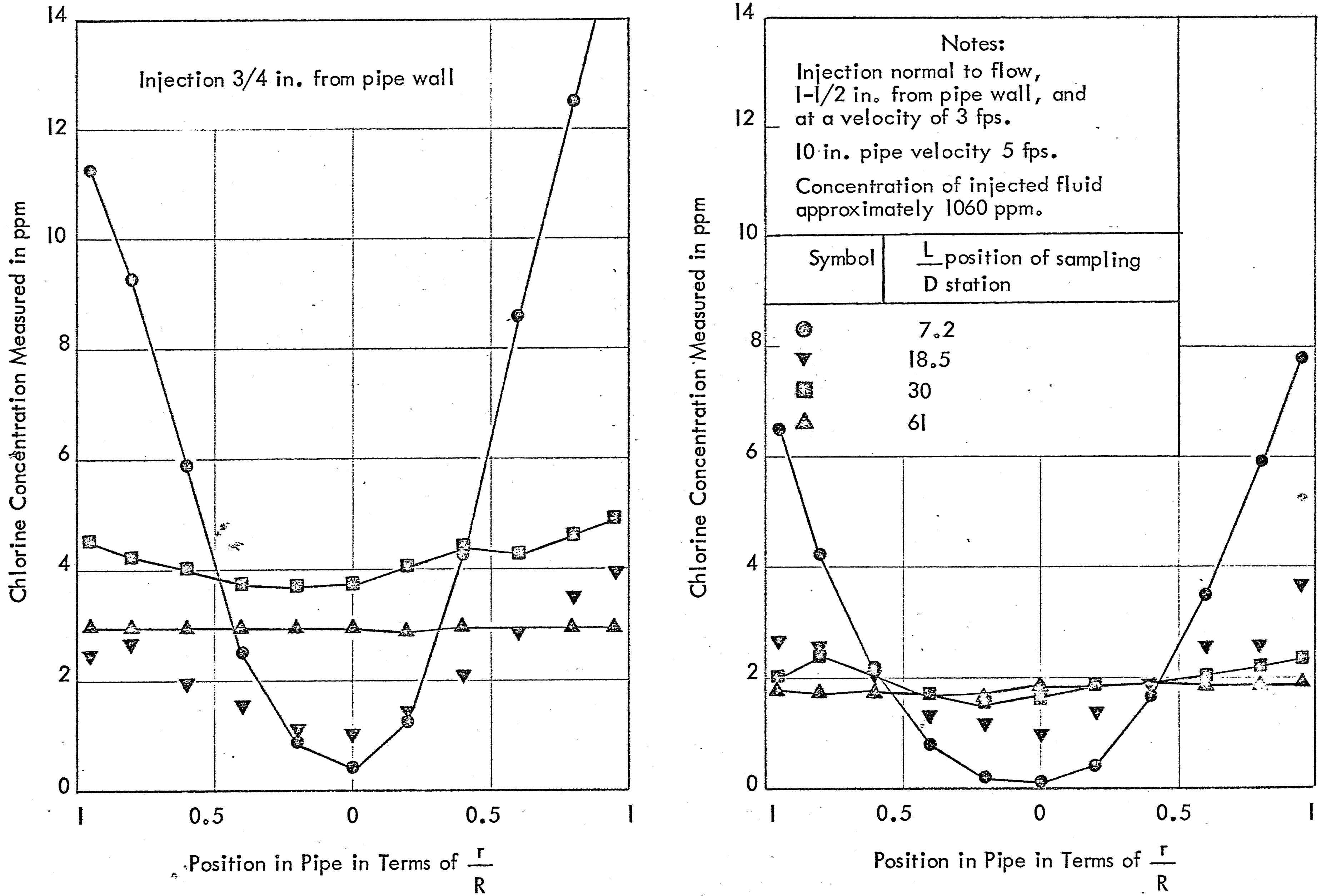

Fig. 12- Concentration Profiles Across the Horizontal Diameter at Various $\frac{L}{D}$ Values Downstream from the Injection Point using two Injectors

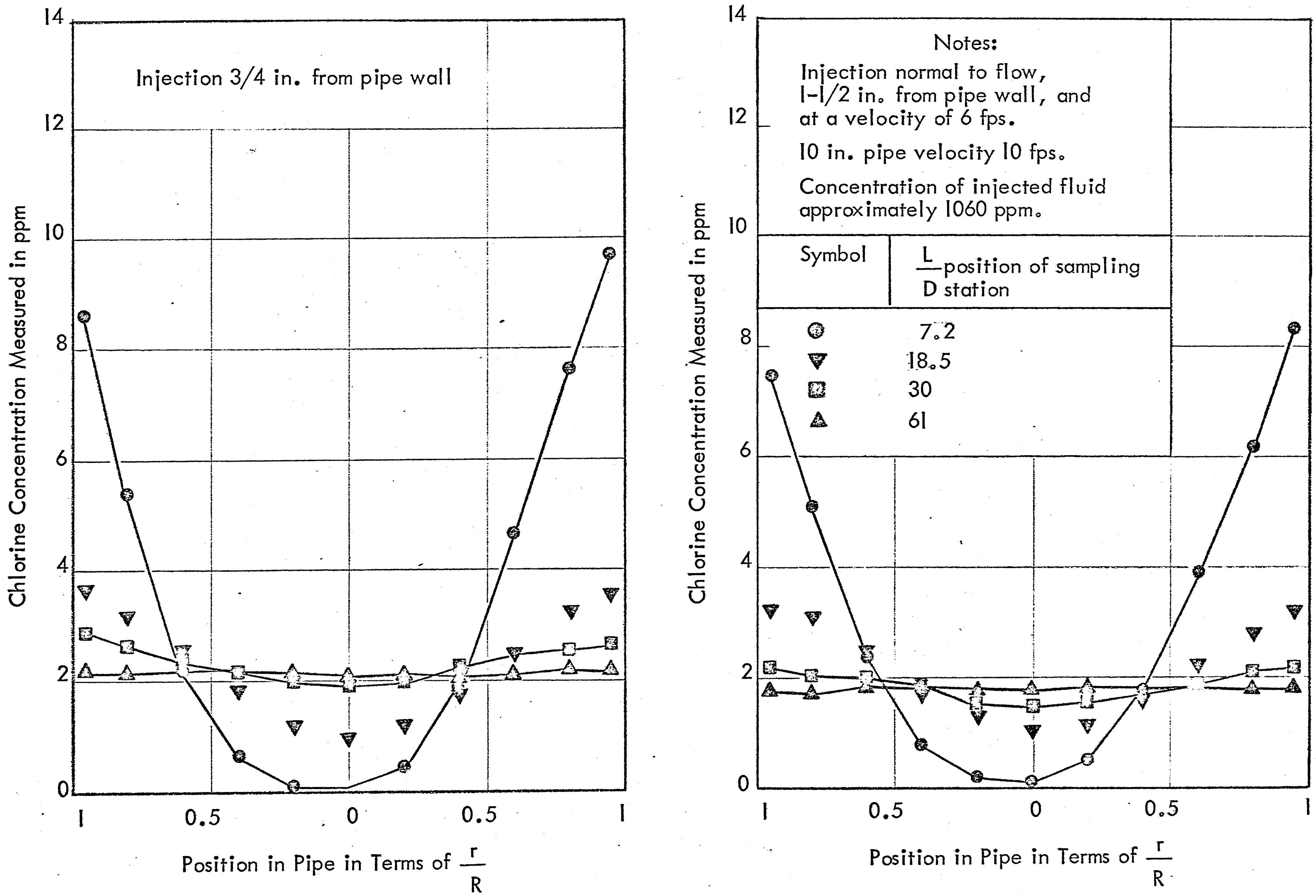

Fig. 13 - Concentration Profiles Across the Horizontal Diameter at Various $\frac{L}{D}$ Values Downstream from the Injection Point using two Injectors

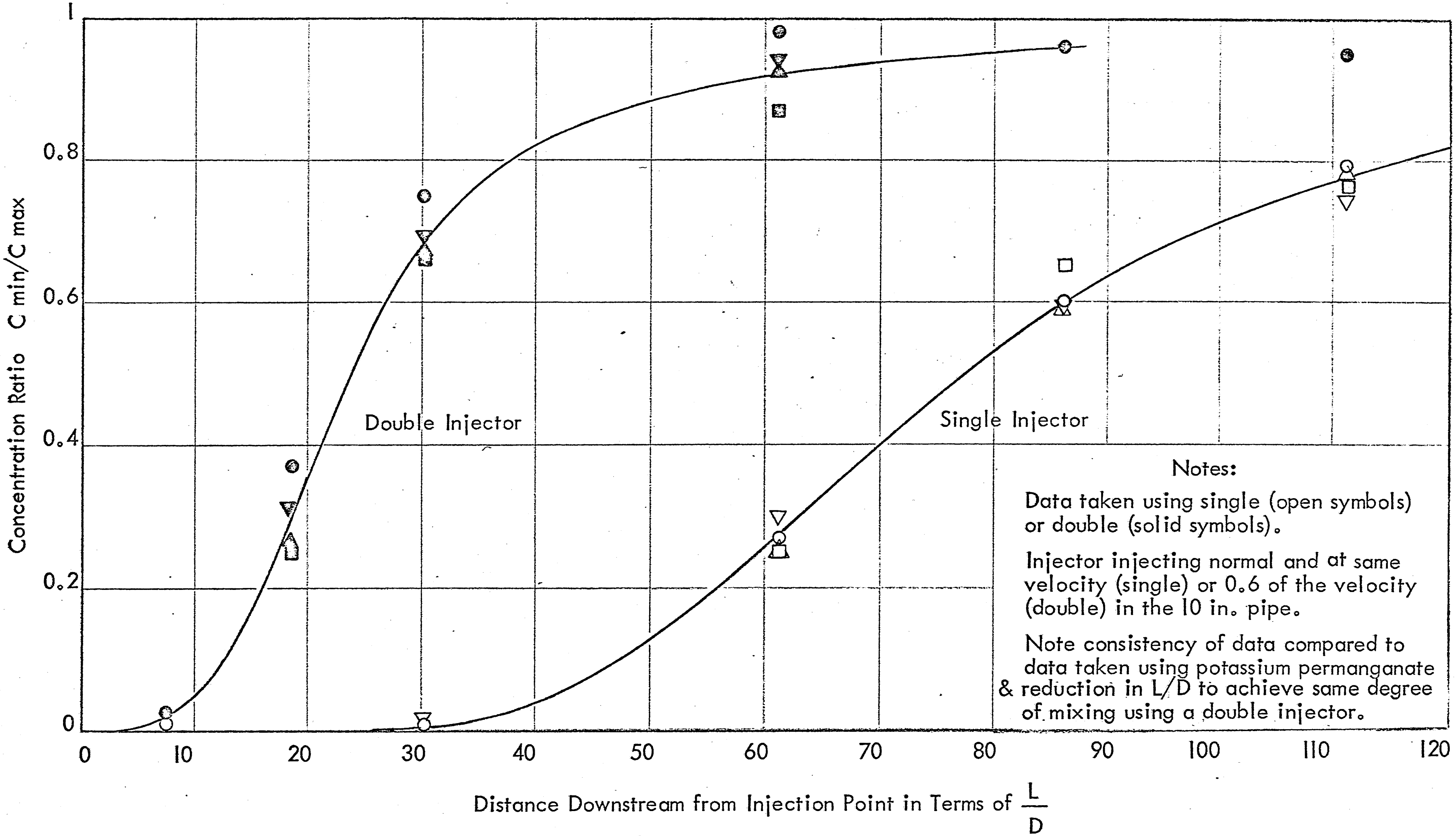

Fig. 14 - C min/C max Ratios at Various $\frac{L}{D}$ Values for the Injection of Chlorine Solution

The Location of the Top of the Pipe in the Prototype Installation is represented by (*) in each of the figures below. Chlorine Concentration Profiles taken across the Horizontal Diameter.

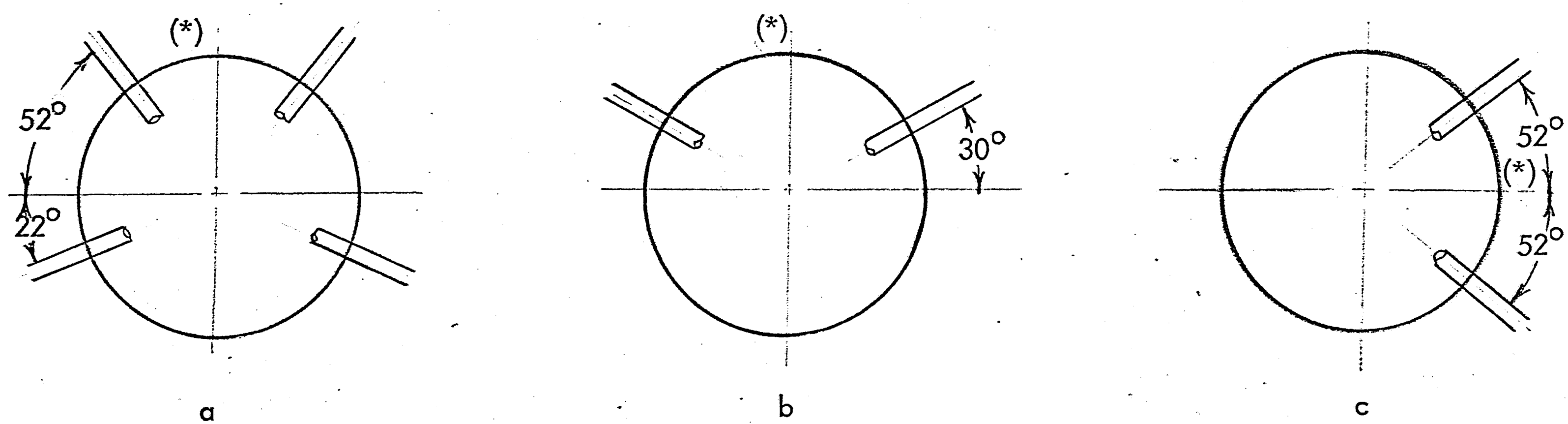

Fig. 15 - Multiple Nozzle Configurations

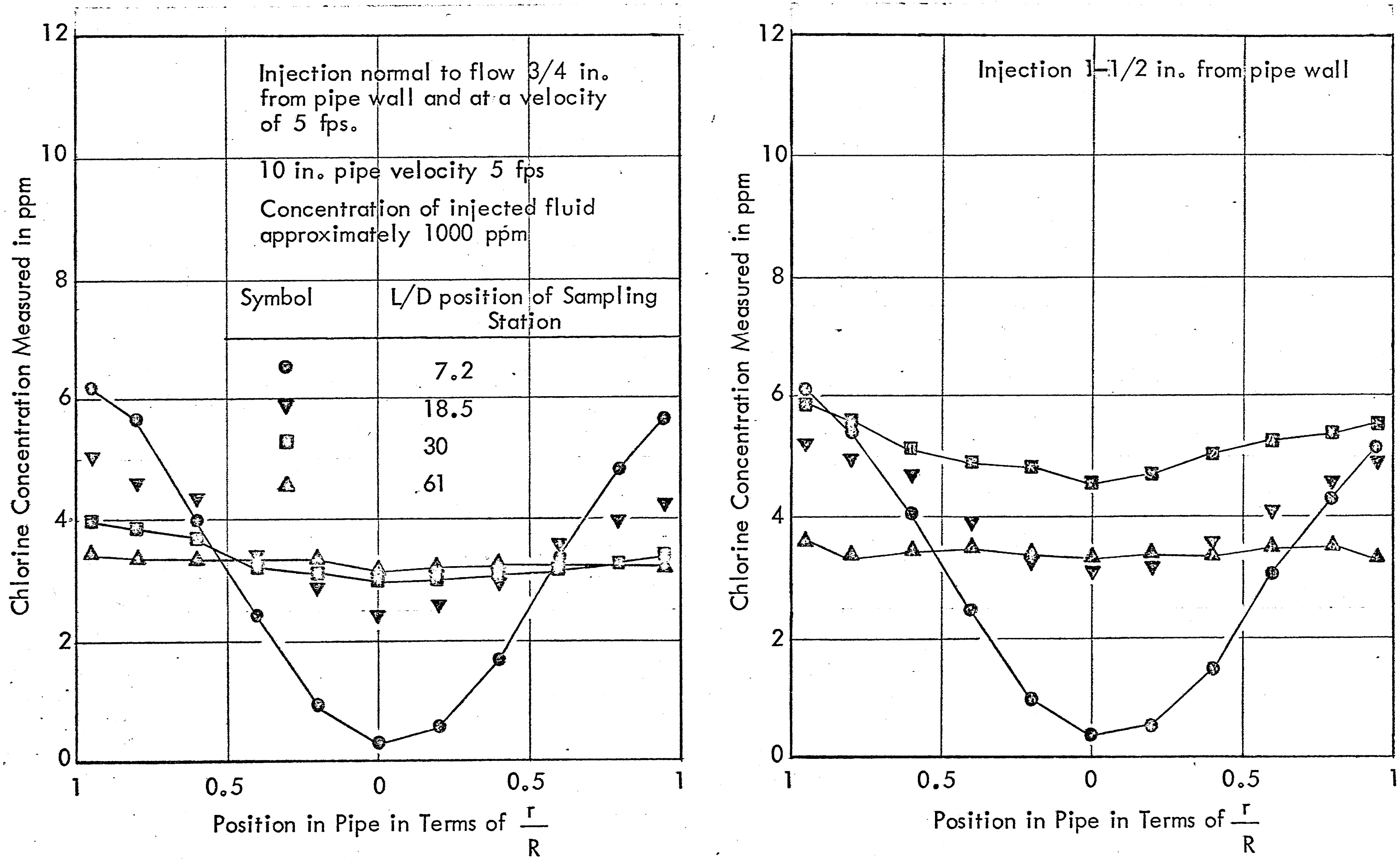

Fig. 16– Concentration Profiles across the Horizontal Diameter at Various L/D Values Downstream from the Injection Point using four Injectors as shown in Fig. 15a.

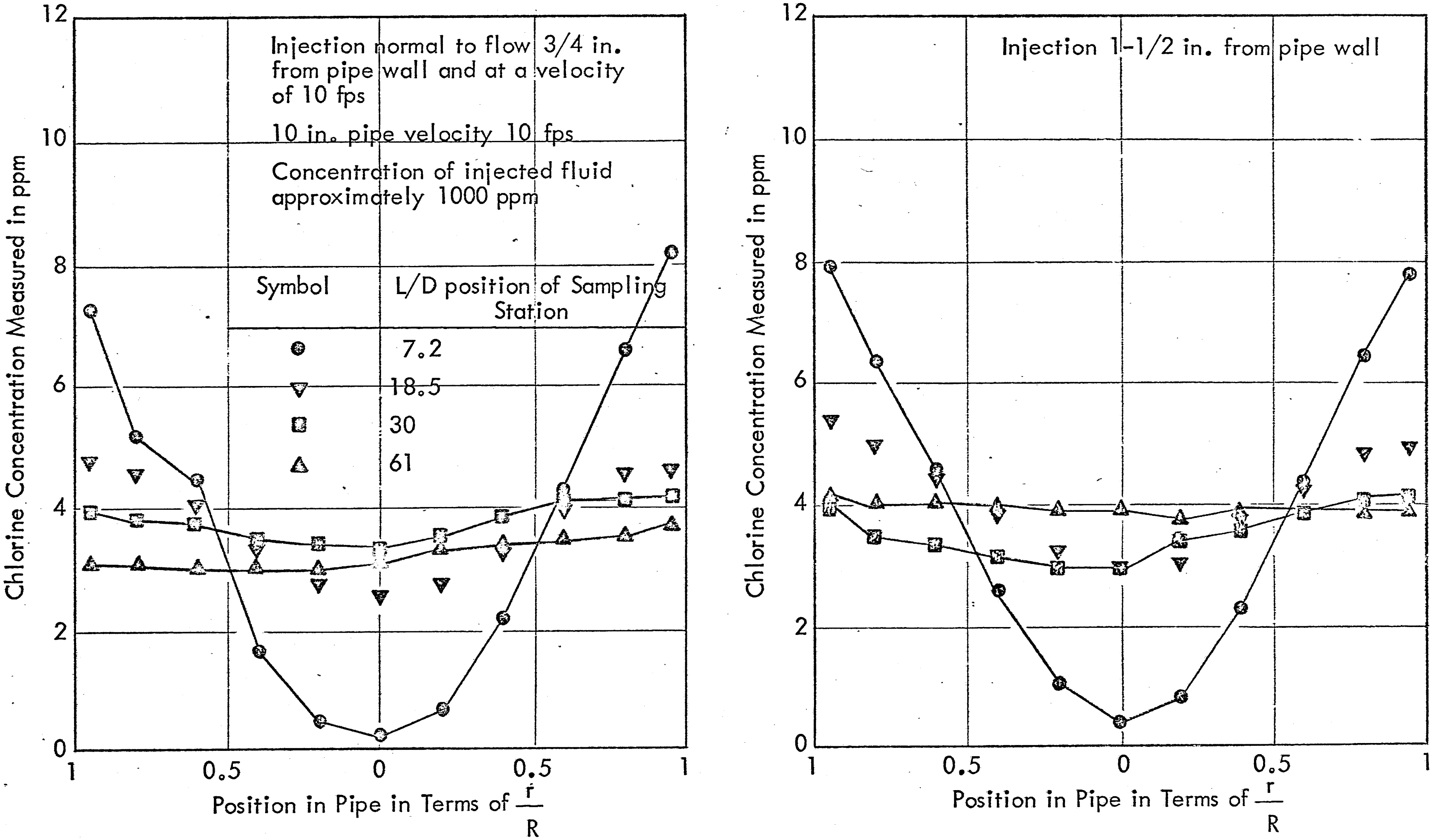

Fig. 17 - Concentration Profiles across the Horizontal Diameter at Various L/D Values Downstream from the Injection Point using four Injectors as shown in Fig. 15 a.

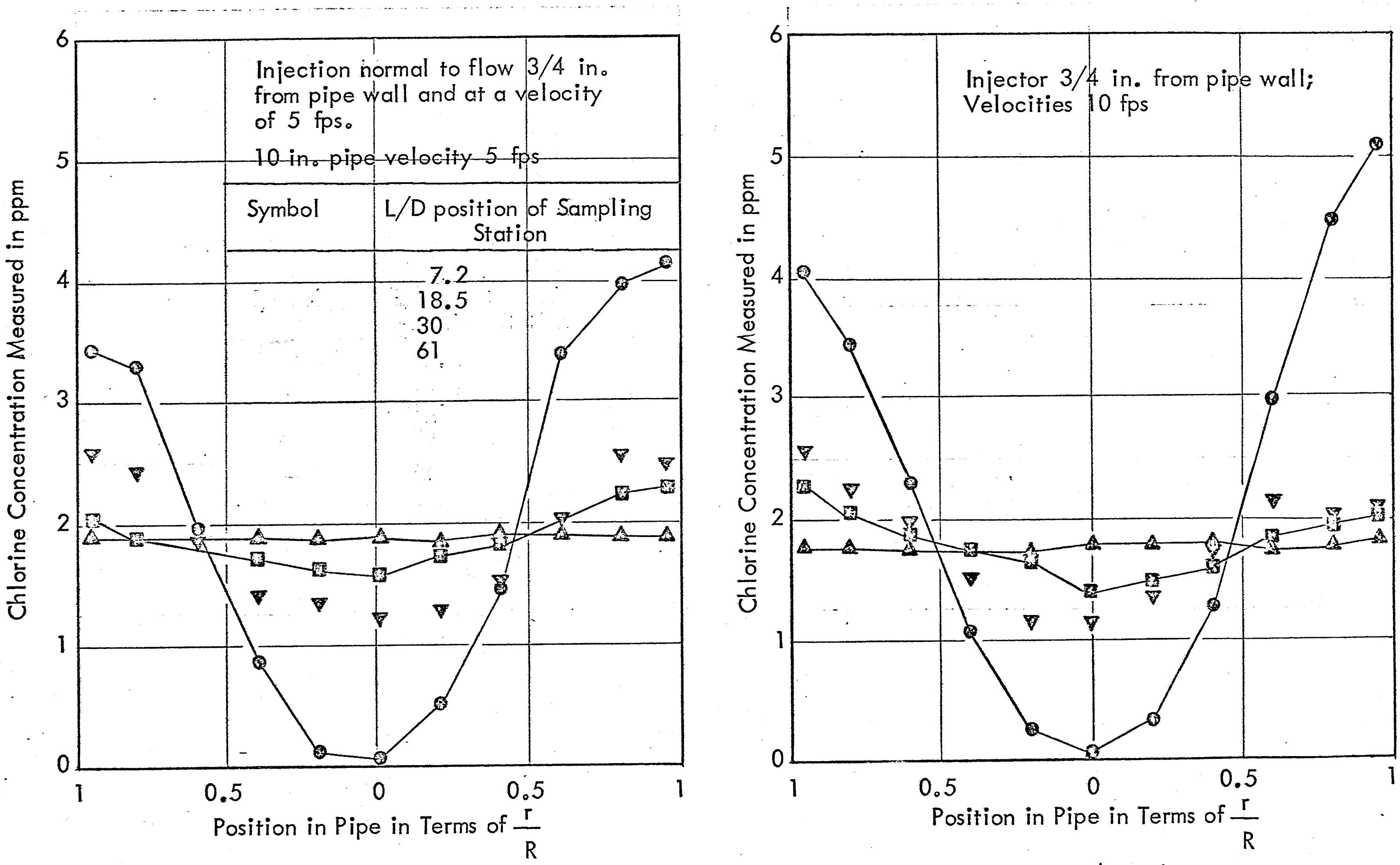

Fig. 18 - Concentration Profiles across the Horizontal Diameter at Various L/D Values Downstream from the Injection Point using two Injectors as shown in Fig. 15b.

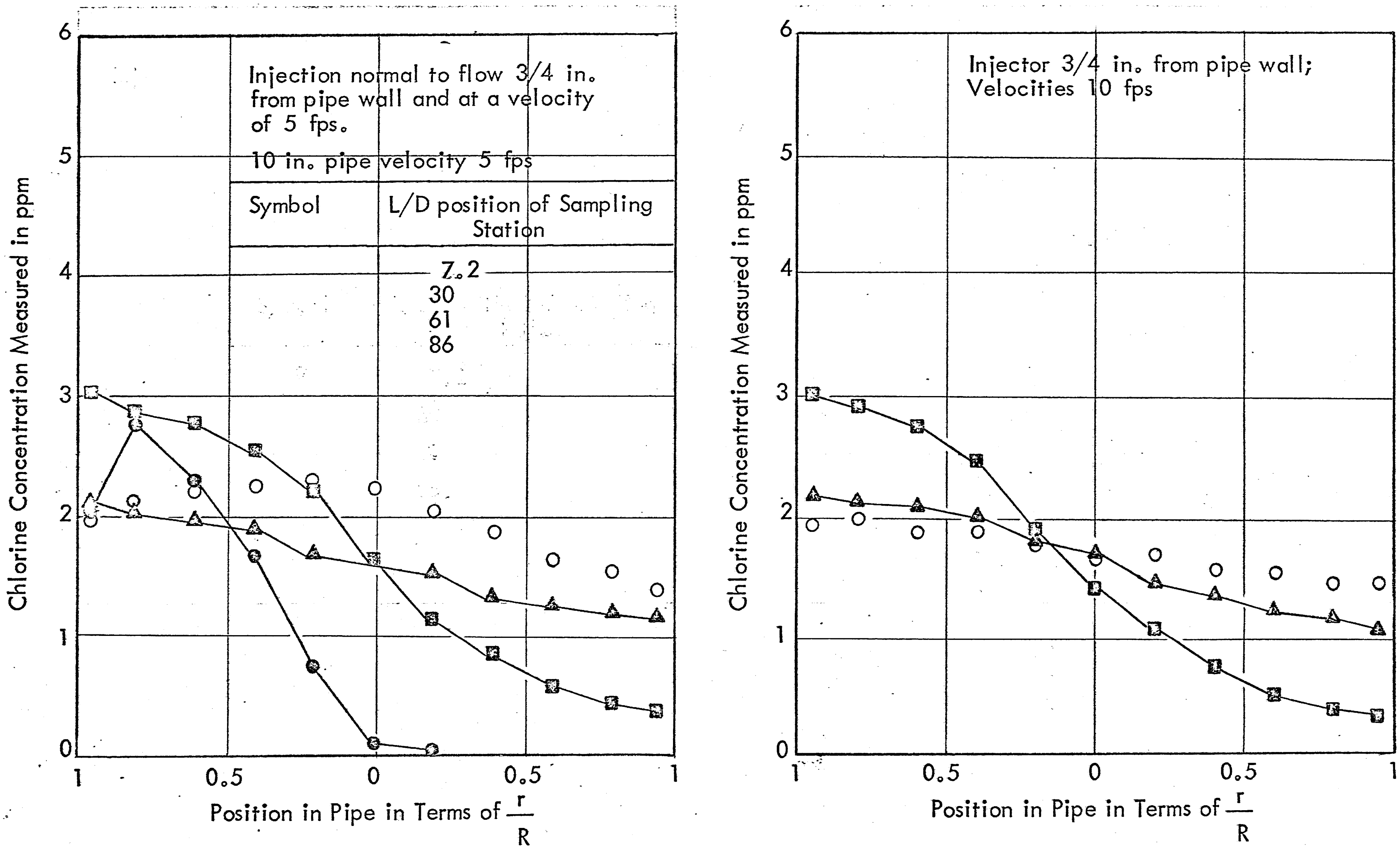

Fig. 19- Concentration Profiles across the Horizontal Diameter at Various L/D Values Downstream from the Injection Point using two Injectors as shown in Fig. 15c.

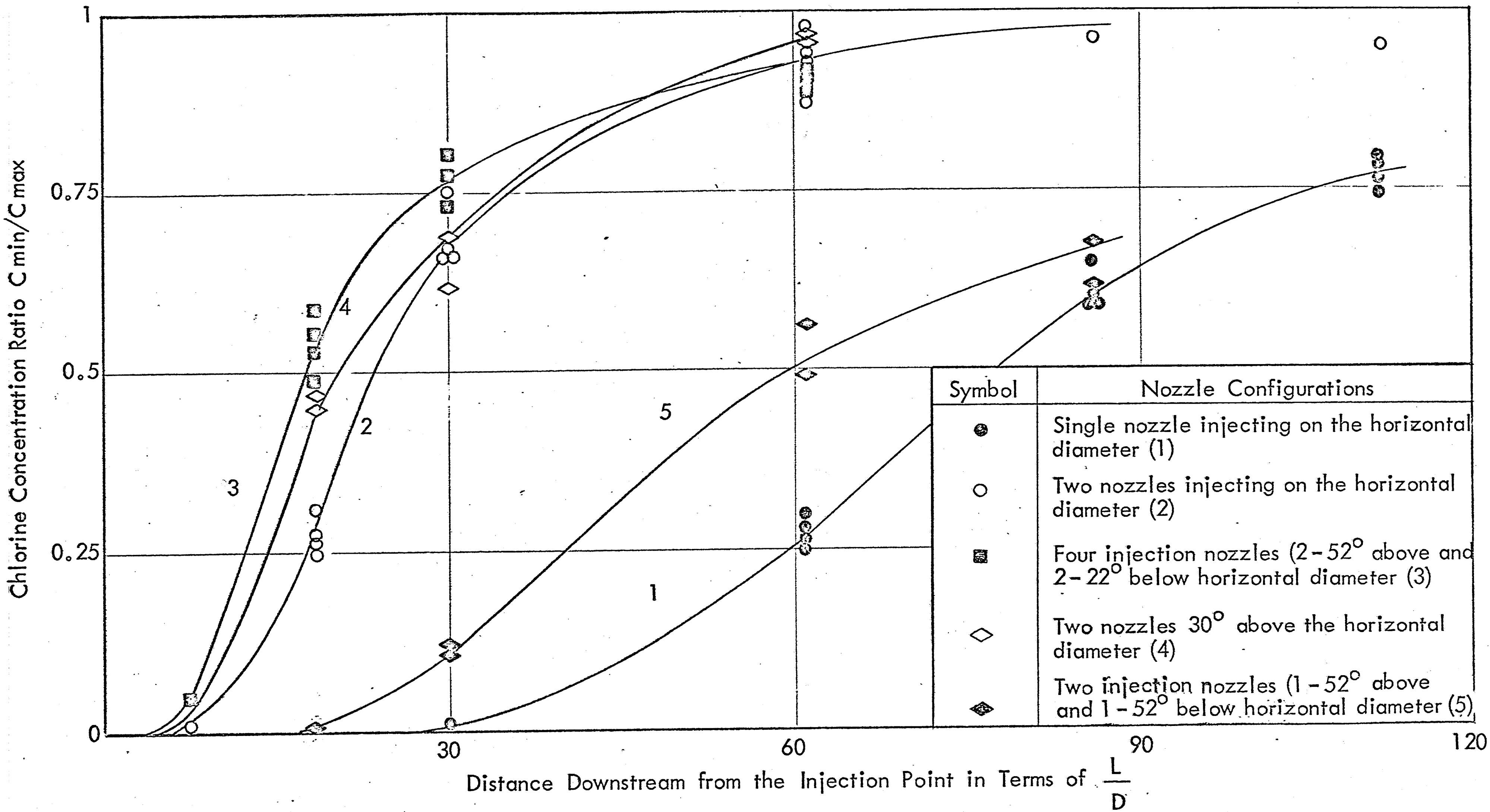

Fig. 20 - Cmin/Cmax Chlorine Concentration Ratios as a Function of the Distance Downstream from the Injection Point for Various Nozzle Configurations

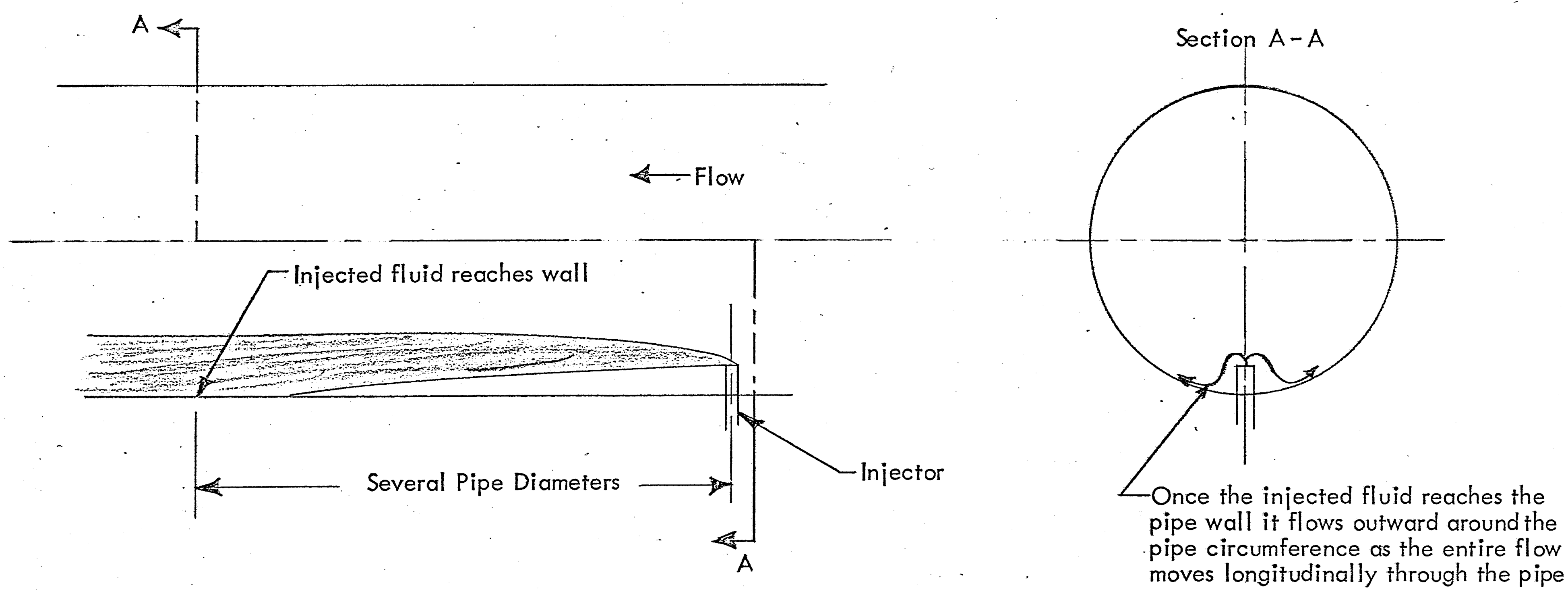

Fig. 21 - Flow Pattern of the Injected Fluid Near the Nozzle